Relating bulk to boundary entanglement

Clément Berthiere[1,*] and William Witczak-Krempa[2,3,†]

[1]*Department of Physics, Peking University, Beijing 100871, China*

[2]*Département de Physique and Regroupement Québécois sur les Matériaux de Pointe (RQMP), Université de Montréal, Montréal, Québec, Canada H3C 3J7*

[3]*Centre de Recherches Mathématiques, Université de Montréal, P.O. Box 6128, Centre-ville Station, Montréal (Québec), Canada H3C 3J7*

(Received 9 August 2019; published 9 December 2019)

Quantum many-body systems have a rich structure in the presence of boundaries. We study the ground states of conformal field theories (CFTs) and Lifshitz field theories in the presence of a boundary through the lens of the entanglement entropy. For a family of theories in general dimensions, we relate the universal terms in the entanglement entropy of the bulk theory with the corresponding terms for the theory with a boundary. This relation imposes a condition on certain boundary central charges. For example, in $2+1$ dimensions, we show that the corner-induced logarithmic terms of free CFTs and certain Lifshitz theories are simply related to those that arise when the corner touches the boundary. We test our findings on the lattice, including a numerical implementation of Neumann boundary conditions. We also propose an ansatz, the boundary extensive mutual information model, for a CFT with a boundary whose entanglement entropy is purely geometrical. This model shows the same bulk-boundary connection as Dirac fermions and certain supersymmetric CFTs that have a holographic dual. Finally, we discuss how our results can be generalized to all dimensions as well as to massive quantum field theories.

DOI: 10.1103/PhysRevB.100.235112

I. INTRODUCTION

Quantum many-body systems are often studied in infinite space or on spaces without boundaries, like tori and spheres, in order to simplify the analysis. However, introducing a boundary is not only more realistic, but it can reveal novel phenomena. For instance, gapped topological phases like quantum Hall states often have protected boundary modes [1]. In fact, such topological boundary modes can often only exist at a boundary of a higher dimensional system. In the gapless realm that will be the focus of this work, boundaries can give rise to novel surface critical behaviors. Generally, many distinct boundary universality classes are possible for a given bulk one, which leads to new critical exponents that are absent in a bulk treatment, see, e.g., Ref. [2].

There has been a recent effort to understand the quantum entanglement properties of critical systems in the presence of a boundary, see, for instance, Refs. [3–12], which provides a new viewpoint compared to the study of correlation functions of local operators. This is partly motivated by the success of entanglement measures in bulk systems. One example is the construction of a renormalization group monotone for relativistic theories in $3d$ (where d stands for the space-time dimension) using the entanglement entropy for certain spatial bipartitions, i.e., the F theorem [13–15]. We recall that the entanglement entropy associated with a pure state $|\psi\rangle$ and a subregion A of the full space $A\cup B$ is defined as $S(A)=-\mathrm{tr}(\rho_A \ln \rho_A)$, where the reduced density matrix is $\rho_A=\mathrm{tr}_B|\psi\rangle\langle\psi|$. An extension of this work to relativistic systems with boundaries results in a new proof of the g theorem in $2d$ [9], and its generalization to higher dimensions [16]. However, the entanglement structure and its dependence on boundary conditions remains largely unknown, the more so for nonrelativistic theories.

In this work, we study the entanglement entropy (and its Rényi generalizations) in ground states of gapless Hamiltonians in the presence of boundaries. An important role will be played by entangling surfaces that intersect the physical boundary. These lead to a new type of corner term that is distinct from the corner terms that have been extensively studied in the bulk. The entanglement entropy of such *boundary corners* has been studied for noninteracting CFTs [8,17,18], certain interacting large-N superconformal gauge theories via the $\mathrm{AdS}_{d+1}/\mathrm{bCFT}_d$ correspondence [19–23], and a special class of Lifshitz theories [24]. For noninteracting CFTs, we find that the boundary corner functions are directly related to the bulk corner function via simple relations. We successfully verify our predictions numerically for the relativistic scalar on the lattice, which requires a numerical implementation of Neumann boundary conditions. For scalar and Dirac CFTs, we show that the boundary corner function can be used to extract certain boundary central charges.

Our paper is organized as follows. After the Introduction, Sec. II introduces the relation between the entanglement entropy of bulk subregions to that of subregions in a theory with a physical boundary. In Sec. III, we study the bulk-boundary relation for regions with corners in (boundary) CFTs, with a focus on free scalars and Dirac fermions. A numerical check on the lattice is presented for the scalar. In Sec. IV, we propose an ansatz in general dimensions, the boundary extensive

*clement.berthiere@pku.edu.cn

†w.witczak-krempa@umontreal.ca

mutual information model, for a CFT with a boundary whose entanglement entropy is purely geometrical. In three space-time dimensions, we obtain the boundary corner function analytically, which gives a certain anomaly coefficient for the theory. In Sec. V, we study the entanglement properties of a gapless noninteracting Lifshitz theory. Using the heat kernel method, we obtain the boundary corner function for both Dirichlet and Neumann boundary conditions, and find that these have the same qualitative features as the relativistic scalar. In Sec. VI, we discuss the extension of our results to massive quantum field theories, focusing on the relativistic scalar. We conclude in Sec. VII with a summary of our main results, as well as an outlook on future research topics. Four appendices complete the paper: Appendix A deals with central charges, Appendix B discusses the entanglement entropy of cylindrical regions in $4d$ space-times for the relativistic scalar, Appendix C shows our implementation of boundary conditions for the discretized scalar field (Dirichlet and Neumann), and Appendix D recalls the high-precision ansatz for the scalar bulk corner function.

II. RELATING BULK TO BOUNDARY ENTANGLEMENT

A. (1 + 1)-dimensional systems

For one-dimensional quantum systems of infinite length described by conformal theories, the n-Rényi entropy, $S_n(A) = \ln(\mathrm{tr}\rho_A^n)/(1-n)$, of an interval of length ℓ takes the form [3,4]

$$S_n(\ell) = \frac{c}{6}\left(1+\frac{1}{n}\right)\ln\frac{\ell}{\epsilon} + 2c_n^0\,, \tag{1}$$

where c is the central charge of the CFT, ϵ is a UV cutoff and c_n^0 is a nonuniversal constant. If the system is not infinite but has a boundary, say it is the semi-infinite line $[0,\infty]$, the Rényi entropies of a finite interval adjacent to the boundary $[0,\ell]$ are now given by [3,4]

$$S_n^{(\mathcal{B})}(\ell) = \frac{c}{12}\left(1+\frac{1}{n}\right)\ln\frac{2\ell}{\epsilon} + \ln g_{\mathcal{B}} + c_n^0\,, \tag{2}$$

where $\mathcal{B}$ is the boundary condition imposed at the origin, c_n^0 is the same [25] nonuniversal constant as in (1), and $\ln g_{\mathcal{B}}$ is the boundary entropy, first discussed by Affleck and Ludwig [26] (see also Refs. [5,6]).

Looking at expressions (1) and (2), one immediately notices that the Rényi entropies for $2d$ CFTs and bCFTs satisfy

$$S_n(2\ell) = 2S_n^{(\mathcal{B})}(\ell)\,, \tag{3}$$

at the leading order in ϵ. Indeed, the logarithmically divergent part of the entropy of an interval in the presence of a boundary can be obtained from the entropy of the union of that interval with its mirror image (with respect to the boundary) in an infinite system, i.e., by the formula (3) for an interval connected to the boundary. In $2d$ bCFTs, the dependence of the n-Rényi entropy on the boundary conditions appears in the subleading terms to the logarithmic divergence, namely, in the boundary entropy $\ln g_{\mathcal{B}}$. Similarly, for d-dimensional CFTs, the presence of a boundary affects the terms subleading to the area law. This means that the analog of formula (3) is valid at the area law level in higher dimensions, but does not necessarily hold for subleading terms, which are the interesting ones as they contain universal information. In this work, we shall show that such a relation between the universal part of the bulk and boundary entanglement entropies does exist in general dimensions. Our results cover not only free CFTs but also certain interacting ones, as well as Lifshitz theories.

B. Free CFTs in general dimensions

For free theories, the n-Rényi entropy may be computed using the heat kernel (or Green function) method together with the replica trick. Essentially, one has to compute the trace of the heat kernel on a manifold with a conical singularity along the entangling surface. Let us take the free scalar field as an example. For a base manifold that is the half-space in $\mathbb{R}^d$, we may impose either Dirichlet or Neumann BCs on the boundary (conformal BCs). The (scalar) heat kernel is then the sum[1] of a "uniform" term, which equals the heat kernel K on $\mathbb{R}^d$ (without boundary), and a "reflected" term K^*. The reflected term satisfies the heat equation, with boundary data canceling that of the uniform term. For Neumann $(+)$ and Dirichlet $(-)$ BCs, one has $K_{N/D} = K \pm K^*$. Taking the trace of these heat kernels one gets $\mathrm{tr}\,K = \widetilde{\mathrm{tr}}(K_N + K_D)$, where tr stands for the trace over $\mathbb{R}^d$ and $\widetilde{\mathrm{tr}}$ for the trace over the half-space only. Thus, considering the entropy of a scalar field for an arbitrary subregion A of $\mathbb{R}^d$ symmetric with respect to some hyperplane, one may obtain the entropy of A as the sum of the Neumann and Dirichlet entanglement entropies of the two mirror subregions with a boundary being the hyperplane of symmetry of A. In $1+1$ dimensions, this reasoning leads to (3) at leading order in ℓ/ϵ for free CFTs, independently of the boundary conditions. As was discussed, this holds for general CFTs in $2d$. These considerations, along with new ones that we shall present in this work, motivate the following conjecture relating bulk and boundary entanglement in $d \geqslant 2$.

C. Bulk-boundary relation

Consider some arbitrary co-dimension 1 spatial region (not necessarily connected) in $\mathbb{R}^{1,d-1}$ which is symmetric with respect to a co-dimension 2 plane. In other words, this region is the union of two mirror symmetric regions A and A', as, for example, shown in Fig. 1. Then, for certain bQFTs, we conjecture that there exist some boundary conditions $\mathcal{B}$ and $\mathcal{B}'$ that may be imposed on the plane of symmetry (physical boundary) such that the following relation between Rényi entropies holds

$$S_n(A\cup A') = S_n^{(\mathcal{B})}(A) + S_n^{(\mathcal{B}')}(A')\,, \tag{4}$$

where $S_n(A\cup A')$ is the n-Rényi entropy for the whole region $A\cup A'$ in the space-time without boundary, while $S_n^{(\mathcal{B})}(A)$ is

[1] In one spatial dimension, the "uniform" term is the well-known solution of the heat equation on $\mathbb{R}$ with initial condition $K(0,x,x') = \delta(x-x')$, i.e. $K(s,x,x') = \frac{1}{\sqrt{4\pi s}}e^{-\frac{1}{4s}(x-x')^2}$, while the "reflected" term is the mirror image through the boundary at, e.g., $x=0$, that is $K^*(s,x,x') = K(s,x,-x')$. Also, $\mathrm{tr}\,K$ is the trace of the heat kernel over the manifold $\mathcal{M}$, $\mathrm{tr}\,K = \int_{\mathcal{M}} dx\, K(s,x,x)$.

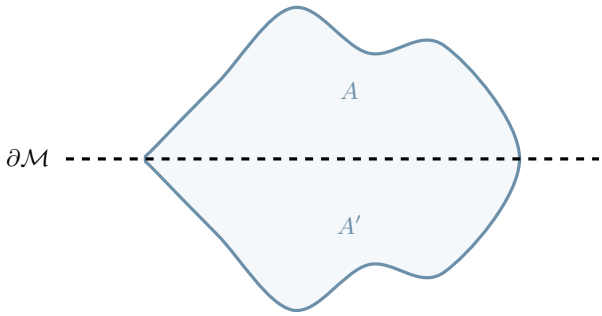

FIG. 1. (b)CFT$_3$ on the (half-) plane. The region A and its mirror image A' with respect to the boundary $\partial\mathcal{M}$ (dashed line) are shown in blue.

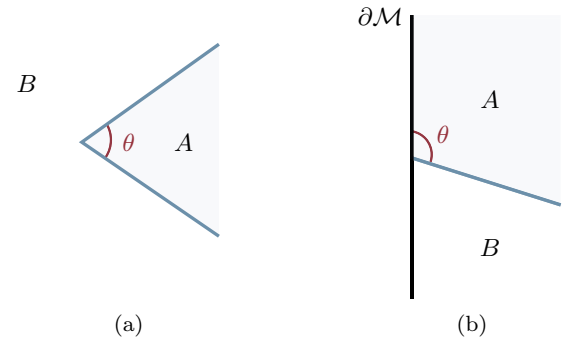

FIG. 2. Spatial partitions of a $(2+1)$-dimensional space $\mathcal{M}$ with boundary $\partial\mathcal{M}$ (black line). (a) The region A is an infinite wedge which presents a bulk corner. (b) The region A is an infinite wedge adjacent to the boundary of the space, and presents a boundary corner.

the n-Rényi entropy for the region A with boundary condition $\mathcal{B}$ imposed on $\partial\mathcal{M}$, and similarly for $S_n^{(\mathcal{B}')}(A')$. One may think that (4) strangely resembles the subadditivity property of an extensive configuration. However, it is not so because we compute entropies for different theories.

A particular case of (4) is given when the boundary conditions coincide, $\mathcal{B} = \mathcal{B}'$:

$$S_n(A \cup A') = 2S_n^{(\mathcal{B})}(A)\,, \tag{5}$$

which can be seen as a generalization of (3). As we shall see, this form of the bulk-boundary entanglement relation will be realized for Dirac fermions, holographic CFTs, and the so-called (boundary) extensive mutual information model.

For $2d$ bCFTs, our relation (4) would imply that $g_{\mathcal{B}'} = g_{\mathcal{B}}^{-1}$ for certain pairs of boundary conditions $\mathcal{B}$, $\mathcal{B}'$. This is actually the case for the XX chain and free fermions with open boundary conditions for which $g_{\mathcal{B}} = 1$ [26,27]. This condition on the boundary entropy can be seen as necessary for the bulk-boundary relation to hold beyond the leading logarithmic term. In higher dimensions, since the leading term in the Rényi entropy is the area law, we expect that the bulk-boundary relation implies a relation for a higher dimensional analogue of the boundary entropy. Let us consider the case of space-time dimension $d = 3$, which will be the focus of the present work. We consider our region A to be a half-disk attached to the physical boundary $\partial\mathcal{M}$. Then its mirror image is also a half-disk, and $A \cup A'$ is a full disk, as illustrated in Fig. 4. The left-hand side of (4) for the ground state of a CFT is then ($n = 1$):

$$S_1(A \cup A') = B\frac{2\pi R}{\epsilon} - F\,, \tag{6}$$

where R is the radius of the disk, and the universal R-independent contribution features the RG monotone in $d = 3$, F. In contrast, the right-hand side of the relation (4) will be built from the half-disk entropy

$$S_1^{(\mathcal{B})}(A) = B\frac{\pi R}{\epsilon} - s_{\log}^{(\mathcal{B})}\ln(R/\epsilon) + \cdots\,, \tag{7}$$

where we have omitted subleading terms in R/ϵ. The logarithmic divergence comes from the two corners generated by the intersection of the entangling surface and the physical boundary. It was argued [8] that $s_{\log}^{(\mathcal{B})}$ is proportional to the boundary central charge $\mathfrak{a}^{\mathcal{B}}$ that appears in the trace of the stress tensor as a consequence of the conformal anomaly. We see that in order for the bulk-boundary entanglement relation (4) at $n = 1$ to hold, the logarithms must cancel, implying:

$$\mathfrak{a}^{\mathcal{B}} + \mathfrak{a}^{\mathcal{B}'} = 0\,. \tag{8}$$

For example, in the case of a free scalar field, the central charges for Dirichlet and Neumann boundary conditions have opposite sign, which is a necessary condition for the relation. If we are dealing with the relation for a single boundary condition $\mathcal{B} = \mathcal{B}'$, (5), this implies that the boundary central charge must vanish, $\mathfrak{a}^{\mathcal{B}} = 0$. This will indeed be the case for Dirac fermions, certain holographic CFTs (with $\alpha = \pi/2$, see below), and the extensive mutual information model. It would be of interest to find which bCFTs obey the relation (8), and the much stronger condition (4). One useful avenue would be to numerically investigate the quantum critical transverse field Ising model in two spatial dimensions along the lines of Ref. [28]. In any case, our conjectured relation (4) provides a useful starting point to compare the bulk and boundary entanglement entropies of QFTs.

III. CFTS IN 2 + 1 DIMENSIONS

In two spatial dimensions, there are many ways to partition a domain. In this paper, we mainly study two different kind of regions that contain corners, and which produce a logarithmic correction to the area law in the entanglement entropy,

$$S = B\frac{\ell}{\epsilon} - s_{\log}(\theta)\ln\frac{\ell}{\epsilon} + \cdots\,, \tag{9}$$

with a certain corner function $s_{\log}(\theta)$ as the cutoff independent coefficient of the logarithmic term. The two corner geometries of interest are depicted in Fig. 2. They may be classified according to whether they touch the boundary of the space (boundary corner), or not (bulk corner).

A. Bulk corners

The first partitioning of the space is the simplest one. The region A is an infinite wedge with interior angle θ, see Fig. 2(a), and thus presents a corner. Let $a(\theta)$ be the bulk

corner function. It only depends on θ, and by purity of the ground state,

$$a(\theta) = a(2\pi - \theta)\,, \tag{10}$$

which allows us to study this corner function for $0 < \theta \leqslant \pi$. The bulk corner function $a(\theta)$ has other interesting properties. It is a positive convex function of θ that is decreasing on $[0, \pi]$ [29], i.e.,

$$a(\theta) \geqslant 0\,, \quad \partial_\theta a(\theta) \leqslant 0\,, \quad \partial_\theta^2 a(\theta) \geqslant 0\,, \tag{11}$$

for $0 < \theta \leqslant \pi$. The behavior of $a(\theta)$ is constrained in the limiting regimes where the bulk corner becomes smooth ($\theta \simeq \pi$), and where it becomes a cusp ($\theta \to 0$):

$$a(\theta \simeq \pi) = \sigma\,(\theta - \pi)^2\,, \quad a(\theta \to 0) = \frac{\kappa}{\theta}\,, \tag{12}$$

where we have introduced two positive coefficients, σ and κ. Furthermore, the smooth bulk corner coefficient σ is universal in the strong sense for general $3d$ CFTs,

$$\sigma = \frac{\pi^2}{24} C_T\,, \tag{13}$$

where C_T is a local observable: the central charge appearing in the two-point function of the stress tensor. This universal relation was conjectured in Refs. [30,31] and subsequently proven in Ref. [32] for general CFTs. Gapless QFTs that are scale and rotationally invariant, but not necessarily conformal, will also receive such a nearly smooth corner contribution to the entanglement entropy. In that case, C_T is replaced by a positive coefficient that appears in the so-called entanglement susceptibility [33].

B. Corners adjacent to the boundary

When the space has a boundary $\partial\mathcal{M}$, one can consider a wedge adjacent to $\partial\mathcal{M}$. In other words, the entangling surface intersects $\partial\mathcal{M}$ with an angle θ, see Fig. 2(b), defining what we call a boundary corner. Then let $b(\theta)$ be the boundary corner function. Depending on the context, we sometimes write $b^{(\mathcal{B})}(\theta)$ making the boundary condition explicit. The boundary corner function depends on the interior angle θ and on the boundary conditions imposed on $\partial\mathcal{M}$. By purity of the vacuum state

$$b(\theta) = b(\pi - \theta)\,, \tag{14}$$

allowing us to only consider $0 < \theta \leqslant \pi/2$. Unlike its bulk counter-part, $b(\theta)$ can be either convex or concave depending on the field theory and the boundary conditions. Its form is also constrained in the orthogonal ($\theta \simeq \pi/2$) and cusp limits:

$$b(\theta \simeq \pi/2) = \eta^{\mathcal{B}} + \sigma^{\mathcal{B}}\,(\pi/2 - \theta)^2\,, \tag{15}$$

$$b(\theta \to 0) = \frac{\kappa^{\mathcal{B}}}{\theta}\,. \tag{16}$$

At exact orthogonality, it was argued that

$$b(\pi/2) = \eta^{\mathcal{B}} \propto \mathfrak{a} \tag{17}$$

is proportional [8,17] to the boundary charge $\mathfrak{a}$ (sometimes called b in the literature) that appears in the conformal anomaly in $3d$. Although not written explicitly here, $\mathfrak{a}$ does depend on the boundary condition $\mathcal{B}$. We refer the reader to Appendix A for further details regarding how the anomaly manifests itself in the trace of the stress tensor in the presence of a boundary. Interestingly, $\mathfrak{a}$ was recently proved to be an RG monotone for boundary RG flows under which the bulk remains critical. However, the coefficient $\eta^{\mathcal{B}}$ is not universal in the strong sense as its value differs for free scalars ($\eta^{\mathcal{B}} = \mathfrak{a}/24$) and for holographic bCFTs[2] ($\eta^{\mathcal{B}} = \mathfrak{a}/96$). Indeed, for holographic bCFTs [21,22], $\eta^{\mathcal{B}}$ comes entirely from the anomaly, whereas for free scalars it is not the case due to the occurrence of the nonminimal coupling of the scalar field to the curvature [8]. In Table I, we summarize our findings for the coefficients appearing in the boundary corner function in the orthogonal and cusp limits for various CFTs, and the $z = 2$ Lifshitz scalar.

TABLE I. Boundary corner coefficients in the orthogonal and cusp regimes for different critical theories. "D/N" stands for Dirichlet/Neumann, while "M" for mixed.

Theory	$\mathfrak{a}^{\mathcal{B}}$	$\eta^{\mathcal{B}}$	$\sigma^{\mathcal{B}}$	$\kappa^{\mathcal{B}}$
Scalar D	1	$1/24$	$3/128$	0.044(4)
Scalar N	-1	$-1/24$	$-1/128$	$-0.024(5)$
Dirac M	0	0	$1/64$	0.0180
$z = 2$ Scalar D	NA	$1/8$	$2/(3\pi^2)$	$\pi/24$
$z = 2$ Scalar N	NA	$-1/8$	$-1/(3\pi^2)$	$-\pi/48$
bEMI	0	0	$s_0 4/3$	$s_0\pi/2$

In this manuscript, we are mostly interested in the logarithmic corner functions that appear in the entanglement entropy for regions as pictured in Fig. 3. Then according to (4), bulk and boundary corner functions should be related to each other through

$$a(2\theta) = b^{(\mathcal{B})}(\theta) + b^{(\mathcal{B}')}(\theta)\,, \tag{18}$$

for some boundary conditions $\mathcal{B}$ and $\mathcal{B}'$ depending on the field theory under consideration. In what follows, we explore the implications of relations (4) and (18) for various models.

[2]Whenever holographic bCFTs are mentioned in the present paper, it refers to Takayanagi's model [19], see Sec. III C.

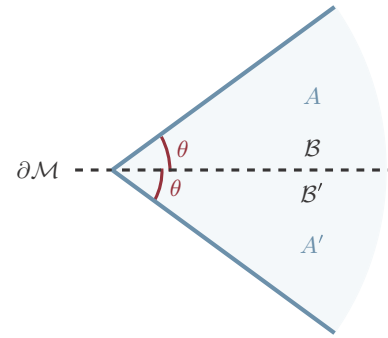

FIG. 3. (b)CFT$_3$ on the (half-)plane. The region A and its mirror image A' through $\partial\mathcal{M}$ each present a boundary corner of opening angle θ, with boundary condition $\mathcal{B}$ and $\mathcal{B}'$, respectively. Their union forms a bulk corner with opening angle 2θ.

C. Holographic theories

Within the AdS/CFT framework, certain holographic CFTs are described by a gravity theory coupled to a negative cosmological constant in one dimension higher. The holographic entanglement entropy (HEE) of some region A in the boundary CFT is computed using the Ryu-Takayanagi prescription [34] as the area (divided by $4G$, where G is the gravitational constant) of the minimal co-dimension 2 surface homologous to A on the conformal boundary of the AdS space-time. The holographic bulk corner function $a_E(\theta)$ for $3d$ CFTs dual to Einstein gravity in AdS_4 has been computed in Refs. [29,35]. The holographic picture of AdS/bCFT was introduced in Ref. [19] and can briefly be sketched as follows. The dual of a $bCFT_d$ is given by a gravity theory in asymptotically AdS_{d+1} space-time restricted by a d-dimensional brane $\mathcal{Q}$ whose boundary coincides with the boundary $\partial\mathcal{M}$ of the $bCFT_d$. The HEE is also computed according to Ryu-Takayanagi prescription. For the simplest geometrical setup in which the boundary of the $bCFT_3$ is flat and its extension $\mathcal{Q}$ into the bulk is completely determined by its slope α, the HEE of an infinite wedge adjacent to the boundary was computed in Ref. [22]. The corresponding boundary corner function $b_E^{(\alpha)}(\theta)$ depends on the extra parameter α, which from a mathematical point of view controls the slope of the brane $\mathcal{Q}$ in the bulk, but from a field theory perspective should be related to the boundary conditions of the underlying holographic theory.

Interestingly, for the value $\alpha = \pi/2$, it has been observed in Ref. [22] that $b_E^{(\pi/2)}(\theta)$ is related to the holographic bulk corner function $a_E(\theta)$ as

$$a_E(2\theta) = 2b_E^{(\pi/2)}(\theta)\,. \tag{19}$$

This equality satisfies our conjecture (4), with boundary conditions given by $\mathcal{B} = \mathcal{B}' : \alpha = \pi/2$. This is the unique set of values of α that leads to the relation (4).

Also shown in Ref. [22] was that the orthogonal-limit boundary coefficient $\sigma_E^{(\alpha)}$ is related to the boundary central charge $A_T^{(\alpha)}$ in the near-boundary expansion of the stress tensor,

$$\sigma_E^{(\alpha)} = -\pi A_T^{(\alpha)}\,, \tag{20}$$

where the general definition of A_T in a $bCFT_d$ is [36]

$$\langle T_{ij}\rangle = \frac{A_T^{(\mathcal{B})}}{\epsilon^{d-1}}\,\hat{k}_{ij}\,, \quad \epsilon \to 0\,. \tag{21}$$

In the above, the stress tensor is inserted at a distance ϵ from the boundary, where we have imposed boundary condition $\mathcal{B}$. $\hat{k}_{ij}$ is the traceless part of the extrinsic curvature tensor of the boundary, k_{ij}. The relation (20) is valid for any value of the continuous parameter α which encodes the BCs in the holographic bCFT. A natural question to ask is whether (20) holds for other theories. We address this question in Sec. III E.

D. Free CFTs

Let us first consider a noninteracting conformal scalar field with Lagrangian density $\mathcal{L} = \frac{1}{2}\partial_\mu\phi\partial^\mu\phi$. Conformal invariance restricts the possible admissible boundary conditions to either Dirichlet or (generalized) Neumann[3] BCs. Then, for free scalars, we conjecture that the bulk corner function $a_s(\theta)$ and the boundary corner function $b_s(\theta)$ are related through

$$a_s(2\theta) = b_s^{(D)}(\theta) + b_s^{(N)}(\theta)\,, \tag{22}$$

where $N(D)$ stands for Neumann(Dirichlet) BCs.

For free Dirac fermions, we consider mixed (M) BCs [37] which yield a vanishing current through the boundary, and where a Dirichlet BC is imposed on a half of the spinor components and a Neumann BC on the other half. With these BCs, the Dirac fermion presents some similarities with scalars evenly split between Neumann and Dirichlet BCs: for example, same structures of certain two-point functions [38,39], also the central charges for the Dirac fermion in the $3d$ anomaly [see (A1)] match the sum of those for Neumann + Dirichlet scalars. We then conjecture the following relation between the bulk corner function $a_f(\theta)$ and the boundary corner function $b_f(\theta)$ for free Dirac fermions:

$$a_f(2\theta) = 2b_f^{(M)}(\theta)\,. \tag{23}$$

This is a special case of (18) with $\mathcal{B} = \mathcal{B}' = M$, similar to that for holographic bCFTs, see (19). Observe that (22) and (23) satisfy the reflection symmetry expected for pure states for $\theta \to \pi - \theta$. Using (12) and (15), in the limit $\theta \simeq \pi/2$, from (22) and (23) we obtain the following relations between the bulk and boundary corner coefficients σ's:

$$4\sigma_s = \sigma_s^D + \sigma_s^N\,, \quad 2\sigma_f = \sigma_f^M\,. \tag{24}$$

We can use the so-called smooth-limit boson-fermion duality [30,40] $\sigma_f = 2\sigma_s$ to get $\sigma_f^M = \sigma_s^D + \sigma_s^N$. One can view this last relation as a new boson-fermion duality in the presence of a boundary, which can be understood heuristically by recalling that a Dirac fermion with mixed BCs has two components, one with Dirichlet BCs and the other one with Neumann BCs. In the opposite regime $\theta \to 0$, inserting (12) and (16) in (22) and (23) yields

$$\kappa_s = 2\left(\kappa_s^D + \kappa_s^N\right), \quad \kappa_f = 4\kappa_f^M\,. \tag{25}$$

Not much is known about $b(\theta)$ for free fields, beyond $\theta = \pi/2$. Only recently [18] has it been computed numerically on the lattice for free scalars with Dirichlet boundary conditions. Numerical values for the two boundary corner coefficients $\sigma^{\mathcal{B}}$ and $\kappa^{\mathcal{B}}$ were found to be $\sigma_s^D = 0.023(4) \simeq 3/128$ and $\kappa_s^D = 0.044(4)$. Then, combining this numerical result for σ_s^D with (24) and the well-known values of the bulk corner smooth-limit coefficients [30,41] $\sigma_s = 1/256$ and $\sigma_f = 1/128$, one can predict the boundary corner orthogonal coefficients to be

$$\sigma_s^D \simeq \frac{3}{128}\,, \quad \sigma_s^N \simeq -\frac{1}{128}\,, \quad \sigma_f^M = \frac{1}{64}\,. \tag{26}$$

For the cusp corner coefficients, we have [41] $\kappa_s = 0.0397$ and $\kappa_f = 0.0722$, which together with $\kappa_s^D = 0.044(4)$ and (25) yield

$$\kappa_s^D = 0.044(4), \quad \kappa_s^N = -0.024(5), \quad \kappa_f^M = 0.0180. \tag{27}$$

[3]Generalized Neumann BC, also called Robin BC, is the generalization of Neumann BC to the case where the boundary has nonvanishing extrinsic curvature.

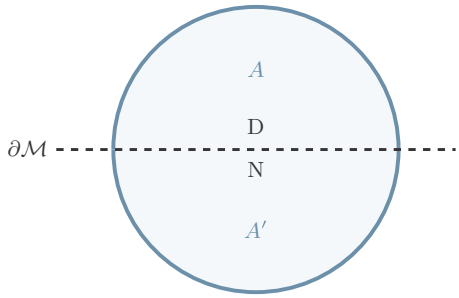

FIG. 4. (b)CFT$_3$ on the (half-) plane. The region A and its mirror image A' through $\partial\mathcal{M}$, shown in light blue, are half-disks orthogonally anchored to $\partial\mathcal{M}$. Their union forms a complete disk.

Further, combining the lattice results of Ref. [18] for Dirichlet scalars for $b_s^{(D)}$ and the exact result of Refs. [41,42] for a_s, we have plotted in Fig. 6 the boundary corner function $b_s^{(N)}$ for Neumann scalars. This function is concave and negative, with a maximum at $\theta = \pi/2$. In the same figure, the boundary corner function for fermions $b_f^{(M)}$ appears, inferred from (23) using the results of Refs. [41,43] for the bulk corner function a_f. Once the functions $b(\theta)$ are properly normalized, as in Fig. 8, the corresponding curves for free scalars evenly split between Dirichlet and Neumann BCs and for free fermions with mixed BCs are very close to each other, as their bulk cousins $a(\theta)$. It will be very interesting to compare these results with direct analytical or numerical calculations of $b_s^{(N)}$ and $b_f^{(M)}$. The numerical lattice calculation of $b_s^{(N)}$ is presented in Sec. III D 2; we find that the relation (22) is indeed obeyed, thus also implying the validity of the values for the boundary coefficients for scalars with Neumann BCs predicted in (26) and (27).

1. Free scalars in the (half-) disk

The Hamiltonian of a free massless real scalar field φ in $2+1$ dimensions reads

$$H = \frac{1}{2}\int d^2x\,(\pi^2 + (\nabla\varphi)^2)\,. \tag{28}$$

We consider a circular region such that we may impose either Dirichlet or Neumann BCs on its diameter, see Fig. 4. In polar coordinates (r,θ), the boundary conditions are imposed at $\theta = 0,\pi$. Due to the symmetries, the fields can be conveniently decomposed in angular modes as

$$\varphi(r,\theta) = \frac{1}{\sqrt{r}}\sum_k f_k(\theta)\,\varphi_k(r)\,, \tag{29}$$

$$\pi(r,\theta) = \frac{1}{\sqrt{r}}\sum_k f_k(\theta)\,\pi_k(r)\,, \tag{30}$$

where $f_k(\theta)$ is a set of orthonormal functions which depend on the BCs such that

$$f_k^{(D)}(\theta) = \sqrt{\frac{2}{\pi}}\sin(k\theta), \quad k = 1,2,\dots\,, \tag{31}$$

$$f_k^{(N)}(\theta) = \sqrt{\frac{2}{\pi}}\cos(k\theta), \quad k = 0,1,\dots\,, \tag{32}$$

with $D\,(N)$ standing for Dirichlet (Neumann) BCs. The Hamiltonian can then be written as $H = \sum_k H_k$, where

$$H_k = \frac{1}{2}\int dr\left(\pi_k^2 + r\partial_r\left(\frac{\varphi_k}{\sqrt{r}}\right)^2 + \frac{k^2}{r^2}\varphi_k^2\right). \tag{33}$$

The entanglement entropies for the half-disk with Dirichlet and Neumann BCs are thus given by

$$S^{(D)}_{\text{h-disk}}(R) = \sum_{k=1}^{\infty} S_k\,, \quad S^{(N)}_{\text{h-disk}}(R) = \sum_{k=0}^{\infty} S_k\,, \tag{34}$$

where S_k is the entropy for the kth mode associated to H_k. Notice that the difference between the entanglement entropy for Dirichlet and Neumann BCs is the presence of the zero mode in the latter,

$$S^{(N)}_{\text{h-disk}}(R) = S_0(R) + S^{(D)}_{\text{h-disk}}(R)\,. \tag{35}$$

It is worth mentioning that the zero mode in $S^{(N)}_{\text{h-disk}}$ contributes a factor of $1/6$ in the logarithmic part of the entropy, while the infinite sum over the higher modes, i.e., $S^{(D)}_{\text{h-disk}}$, contributes negatively with $-1/12$.

Now, we want to compute the entanglement entropy of a complete disk of radius R (no boundary here). Just as before, we can take advantage of the rotational symmetry and decompose the fields on angular modes, with eigenfunctions $f_k(\theta) = \frac{1}{\sqrt{2\pi}}e^{ik\theta}$, where $k \in \mathbb{Z}$. One then finds that the entanglement entropy of a disk is given by

$$S_{\text{disk}}(R) = \sum_{k=-\infty}^{\infty} S_k = S_0 + 2\sum_{k=1}^{\infty} S_k\,. \tag{36}$$

Comparing (36) to (35), one obtains

$$S_{\text{disk}}(R) = S^{(D)}_{\text{h-disk}}(R) + S^{(N)}_{\text{h-disk}}(R)\,, \tag{37}$$

which is exactly our conjectured relation (4), applied to the (half-) circle for the scalar field with Dirichlet/Neumann BCs. Let us emphasize that (37) is valid for the full entropies, including the finite terms. These finite contributions, let us denote them $-F_{D/N}$, are unphysical by themselves as they may be spoiled by the logarithmic term upon rescaling the UV regulator. Their sum, however, is a physical quantity $F_D + F_N = F$, that is the free energy on $\mathbb{S}^3$, see (6).

One can also check that (37) yields a consistent relation for the corner functions:

$$a_s(\pi) = b_s^{(D)}(\pi/2) + b_s^{(N)}(\pi/2) \quad \Leftrightarrow \quad 0 = \frac{1}{24} + \frac{-1}{24} = 0\,. \tag{38}$$

Similar calculations can be done for a scalar field in a cylinder in $4d$ (see Appendix B) or in the $(d-2)$-sphere, see, e.g., Refs. [44,45].

2. Lattice calculations for the free scalar

We consider the discretized Hamiltonian of a $(2+1)$-dimensional free massless scalar field on a square lattice given by

$$H = \frac{1}{2}\sum_{x,y}\left[\pi_{x,y}^2 + (\phi_{x+1,y} - \phi_{x,y})^2 + (\phi_{x,y+1} - \phi_{x,y})^2\right], \tag{39}$$

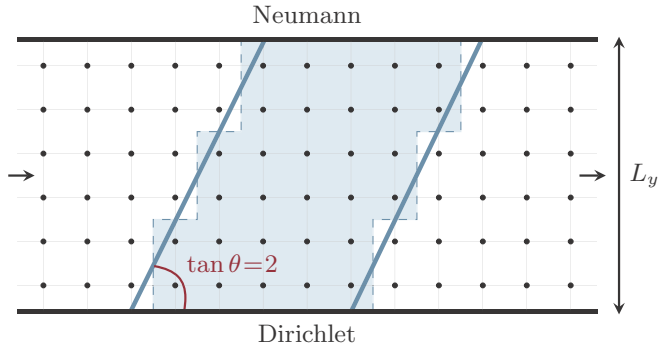

FIG. 5. Two-dimensional square lattice with Dirichlet-Neumann BCs imposed in the (vertical) y direction and PBCs in the (horizontal) x direction. The region A is shown in blue and has $L_x^A = 5$. The entangling surface intersects the boundaries with angles $\theta = \arctan(\pm 2)$.

where $\mathbf{x} = (x, y)$ represents the spatial lattice coordinates with $x_i = 1, \ldots, L_i$, and L_i is the lattice length along the ith direction. The total number of sites is $N = L_x L_y$. The Hamiltonian (39) corresponds to a lattice of coupled quantum harmonic oscillators, and its linearly dispersing acoustic mode is described by the free scalar CFT. H may also be written more compactly as

$$H = \frac{1}{2}\sum_{\mathbf{x}} \pi_{\mathbf{x}}^2 + \frac{1}{2}\sum_{\mathbf{x},\mathbf{x}'} \phi_{\mathbf{x}} K_{\mathbf{x}\mathbf{x}'} \phi_{\mathbf{x}'}, \tag{40}$$

where K is an $N \times N$ matrix encoding the nearest-neighbor interactions between lattice sites as well as the boundary conditions. The vacuum two-point correlation functions $X_{\mathbf{x}\mathbf{x}'} \equiv \langle \phi_{\mathbf{x}} \phi_{\mathbf{x}'} \rangle$ and $P_{\mathbf{x}\mathbf{x}'} \equiv \langle \pi_{\mathbf{x}} \pi_{\mathbf{x}'} \rangle$ are given in terms of the matrix K by

$$X = \frac{1}{2} K^{-1/2}, \quad \text{and} \quad P = \frac{1}{2} K^{1/2}. \tag{41}$$

The entanglement entropy can then be calculated [41] from the eigenvalues ν_ℓ of the matrix $C_A = \sqrt{X_A P_A}$, where X_A and P_A are the correlation matrices restricted to the region A:

$$S(A) = \sum_\ell \left[\left(\nu_\ell + \frac{1}{2}\right) \ln\left(\nu_\ell + \frac{1}{2}\right) - \left(\nu_\ell - \frac{1}{2}\right) \ln\left(\nu_\ell - \frac{1}{2}\right) \right]. \tag{42}$$

We choose to impose periodic BC in the x direction and Dirichlet-Neumann BCs in the y direction, i.e., $\phi_{L_x+1,y} = \phi_{1,y}$, and $\phi_{x,0} = 0$ and $\phi_{x,L_y+1} - \phi_{x,L_y} = 0$. Note that the Dirichlet-Neumann BCs do not have the zero mode that would have been present for Neumann-Neumann. We compute the entanglement entropy for regions A of width L_x^A with fixed ratio $L_x^A/L_y = 4$, as depicted in Fig. 5, and extract the logarithmic contribution by performing least-squares fits of our numerical data to the scaling ansatz [41,42,46,47]

$$S(L_y) = s_1 L_y - 2 s_{\log} \ln L_y + s_0 + s_{-1} L_y^{-1} + \cdots + s_{-p_{\max}} L_y^{-p_{\max}}. \tag{43}$$

For the Dirichlet-Neumann BCs that we have chosen, the region A displays four boundary corners; two Dirichlet and two Neumann (the factor two is due to the symmetry $b(\theta) = b(\pi - \theta)$). The logarithmic contribution $2s_{\log}$ in the entropy is thus the sum of the Dirichlet and Neumann boundary corners functions, such that once extracted, we may directly check our conjectured relation (22) as

$$s_{\log} = b^{(D)}(\theta) + b^{(N)}(\theta) \stackrel{?}{=} a(2\theta). \tag{44}$$

We present in Appendix C the implementations of different boundary conditions on a one-dimensional lattice, and in particular Neumann BC. The extension to higher dimensional lattices is straightforward. The two-dimensional vacuum two-point functions in the thermodynamic limit $L_x \to \infty$ are the following:

$$\langle \phi_{i,j} \phi_{r,s} \rangle = \frac{\binom{i-r-1/2}{i-r}}{L_y + 1/2} \sum_{k_y} \sin(k_y j) \sin(k_y s) \times \sqrt{\frac{z^{2(i-r)+1}}{1-z^2}}\, {}_2F_1\left(\frac{1}{2}, \frac{1}{2}; i-r+1; \frac{z^2}{z^2-1}\right), \tag{45}$$

$$\langle \pi_{i,j} \pi_{r,s} \rangle = \frac{\binom{i-r-3/2}{i-r}}{L_y + 1/2} \sum_{k_y} \sin(k_y j) \sin(k_y s) \times \sqrt{\frac{1-z^2}{z^{2(i-r)+1}}}\, {}_2F_1\left(-\frac{1}{2}, \frac{3}{2}; i-r+1; \frac{z^2}{z^2-1}\right), \tag{46}$$

where we defined $z = (|\sin(k_y/2)| - \sqrt{\sin^2(k_y/2) + 1})^2$ with $k_y = \pi(2n_y - 1)/(2L_y + 1)$ and $n_y = 1, \ldots, L_y$. Expressions (45) and (46) are the matrix elements of the correlation matrices X_A and P_A, respectively [where (i, j) and (r, s) are the raw and column indices, respectively]. On square lattices, angles which obey $\tan\theta = r \in \mathbb{Q}$ are accessible by "pixelation" of the region A (see, e.g., Refs. [18,46]). This is shown in Fig. 5 for $\tan\theta = \pm 2$. Our lattice results for the free scalar with Dirichlet-Neumann BCs are given in Table II in which we have reported the digits that we found to be robust. We also include in this table the values of $a(2\theta)$ from the "high-precision ansatz" of Ref. [46] (see Appendix D), the numerical results of Ref. [18] for $b^{(D)}(\theta)$, as well as the values of $b^{(N)}(\theta)$ deduced from the previous results. Plots of all this are shown in Fig. 6.

As can be seen in Table II, we find a difference of less than 0.5% between our numerical results for $b^{(D)}(\theta) + b^{(N)}(\theta)$ and the field theoretic ones [46] for $a(2\theta)$, thus implying the validity of (22). The high-precision lattice results [46] for the bulk corner function $a(2\theta)$ are also in close agreement with our numerical results; we do not show their values here since they agree with the field theoretic ones within error bars. Further, we have computed the $n = 2$ Rényi entropy and find that (22) also holds in that case within less than 1% discrepancy between the numerics and the theory. Table II shows the comparison with the high-precision field theory results for $a_2(2\theta)$ [46].

Using our numerical results, we find that the Rényi index n and the angle dependences in the entropy do not factorize. If it were the case, we would have $b_n(\theta)/b(\theta) = \text{const}$ valid for all angles θ. This ratio for $n = 2$ shows a deviation of 13%

TABLE II. Lattice results for the boundary corner entanglement for free scalars. The second column presents our numerical results for $b^{(D)}(\theta)+b^{(N)}(\theta)$, which we compare to those of Ref. [46] for $a(2\theta)$ in the third column. In the fourth column, the numerical results of $b^{(D)}(\theta)$ are reported [18]. Next, we give values of the Neumann boundary corner function $b^{(N)}(\theta)=a(2\theta)-b^{(D)}(\theta)$. The next two columns compare our numerical results for the $n=2$ Rényi case $b_2^{(D)}(\theta)+b_2^{(N)}(\theta)$ with the theoretical one $a_2(2\theta)$ of Ref. [46]. We also give $b_2^{(D)}(\theta)$, which was computed using a lattice with DD boundary conditions. The last column shows $b_2^{(N)}(\theta)=a_2(2\theta)-b_2^{(D)}(\theta)$.

n	Entanglement entropy $n=1$				Rényi entropy $n=2$			
$\tan\theta$	$b^{(D)}(\theta)+b^{(N)}(\theta)$	$a(2\theta)$ [46]	$b^{(D)}(\theta)$ [18]	$b^{(N)}(\theta)$	$b_2^{(D)}(\theta)+b_2^{(N)}(\theta)$	$a_2(2\theta)$ [46]	$b_2^{(D)}(\theta)$	$b_2^{(N)}(\theta)$
1/4	0.0730	0.0730(6)	0.182(4)	−0.109(4)	0.0412	0.04127	0.1340	−0.0927
1/2	0.0319	0.03195	0.09798	−0.0660	0.0177	0.01779	0.07223	−0.05444
1	0.0118(3)	0.011833	0.06081	−0.04898	0.00648	0.006487	0.04511	−0.03862
2	0.00357	0.003579	0.04717	−0.04359	0.00194	0.001943	0.03522	−0.03327
4	0.00095	0.000953	0.04310	−0.04215	0.00051	0.000516	0.03228	−0.03177
∞	10^{-7}	0	$\sim 1/24$	$\sim -1/24$	10^{-8}	0	$\sim 1/32$	$\sim -1/32$

for Neumann BCs, and only 2% for Dirichlet BCs between $\theta=\pi/2$ and $\theta=\arctan(1/4)$. At orthogonality, our results for $n=1,\,2$ are in perfect agreement with the following relation [8,17]:

$$b_n(\pi/2)=\frac{1}{2}\left(1+\frac{1}{n}\right)b(\pi/2)\,, \tag{47}$$

where $b(\theta)\equiv b_1(\theta)$. This can be understood by using the replica trick. The Rényi entropies may be computed by introducing in the underlying manifold a conical singularity located at the entangling surface. In three dimensions, when a flat entangling curve intersects orthogonally the flat physical boundary, the singular space-time factorizes as the product of a two-dimensional cone (the singular part, n-dependent) with a semi-infinite interval (the entangling line). As a result, the Rényi entropy is simply proportional to the entanglement entropy, hence (47). Now if the entangling curve is not orthogonal to the boundary, we do not have a product space, therefore the Rényi index n and the angle dependences in the entropy do not factorize, as we verified numerically.

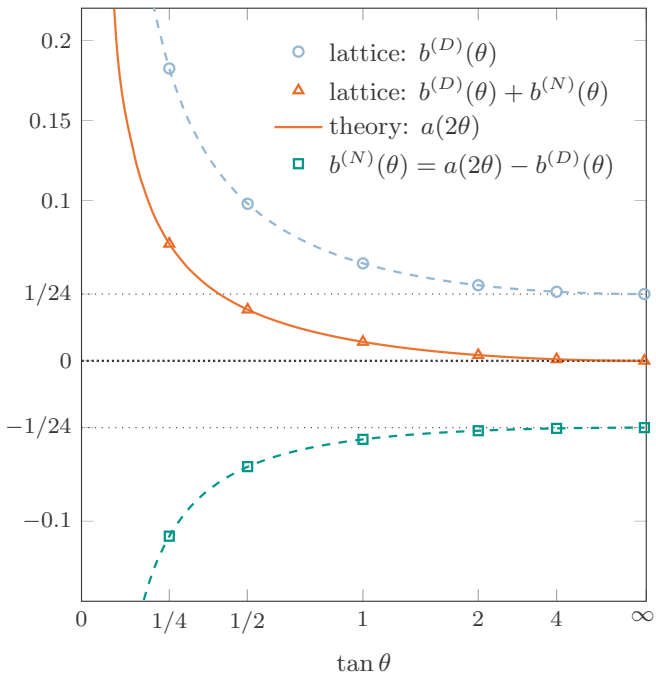

FIG. 6. Corner entanglement for free scalars. The orange triangles are our numerical results for $b^{(D)}(\theta)+b^{(N)}(\theta)$, while the solid orange line is the "high-precision ansatz" of Ref. [46] for $a(2\theta)$. The numerical results for $b^{(D)}(\theta)$ found in Ref. [18] are the blue circles. With green squares are shown the values of the Neumann boundary corner function as deduced from $b^{(N)}(\theta)=a(2\theta)-b^{(D)}(\theta)$. Finally, the dashed blue and green lines are interpolations of the numerical data.

E. Relation to central charges

It has been conjectured in Ref. [18] that relation (20) should hold for free scalars split evenly between Neumann and Dirichlet BCs, and for free fermions with mixed BCs, due to properties that these theories share with the holographic one at $\alpha=\pi/2$. For scalars, the value of A_T^s for both BCs is known, $A_T^{s,D}=A_T^{s,N}=-1/(128\pi)$, which is actually independent of the boundary condition. The expression corresponding to (20) for Dirichlet + Neumann scalars reads

$$\left(\sigma_s^D+\sigma_s^N\right)/2=-\pi A_T^s\,, \tag{48}$$

and is indeed satisfied with the values of $\sigma_s^{D/N}$ given in (26). Note that (20) does not hold for free scalars with Dirichlet *or* Neumann BCs alone [18]. The value of A_T for fermions is known through its relation with the boundary central charge c in the trace anomaly [48] (see Appendix A), $A_T^f=-1/(64\pi)=2A_T^s$ hence

$$\sigma_f^M=-\pi A_T^f \tag{49}$$

holds for fermions as well, using $\sigma_f^M=1/64$ predicted in (26). As we will see shortly, this may be understood as a consequence of A_T being related to C_T for free scalars and fermions. The validity of $\sigma^{\mathcal{B}}=-\pi A_T$ for free Dirichlet-Neumann scalars, mixed fermions and holographic theories dual to Einstein gravity raises the question whether it also holds for other $3d$ theories with appropriate BCs. It would be interesting to test this hypothesis with different models in order to see if universality is indeed at play here.

Now, recall that for bulk corners, the smooth-limit coefficient σ is universal and proportional to C_T, see (13). Then, using (13) and (24) together with (48) and (49) yields the relation

$$A_T=-\frac{\pi}{12}C_T\,. \tag{50}$$

One can check that this equality indeed holds for scalars with $A_T^s = -1/(128\pi)$ and $C_T^s = 3/(32\pi^2)$, and for fermions using $A_T^f = -1/(64\pi)$ and $C_T^f = 3/(16\pi^2)$. We thus find through the connection between bulk and boundary corner entanglement that the charge A_T appearing in the near-boundary expansion of the stress tensor is in fact related to C_T, and it appears so in a universal way for free fields. In fact, such a relation between A_T and C_T seems to exist in any dimensions for free fields, and for holographic theories with BC $\alpha = \pi/2$ only [49], see Appendix A for further details.

We also notice that with (26), the boundary corner coefficients for free fields may be expressed in a universal form

$$\sigma^{\mathcal{B}} = \frac{\pi^2}{12} C_T + \frac{\mathfrak{a}}{64} = -\pi A_T + \frac{\mathfrak{a}}{64}\,, \tag{51}$$

where $\mathfrak{a}$ is the boundary central charge in the conformal anomaly (see Appendix A): $\mathfrak{a} = \pm 1$ for scalars with Dirichlet (+) and Neumann (−) BCs, and $\mathfrak{a} = 0$ for fermions with mixed BCs. Note that (51) is not valid for holographic bCFTs with arbitrary α, but it does hold for $\alpha = \pi/2$ (the charge $\mathfrak{a} \propto \cot\alpha$ vanishes in that case).

IV. EXTENSIVE MUTUAL INFORMATION MODEL

Within the extensive mutual information model (EMI) [50–52], the entanglement entropy of a region A in infinite flat space is obtained by the following double integral over two copies of the boundary ∂A of A:

$$S_{\rm EMI}(A) = s_0 \int_{\partial A} d\mathbf{r}' \int_{\partial A} d\mathbf{r}\, \frac{\hat{n}\cdot\hat{n}'}{|\mathbf{r}'-\mathbf{r}|^{2(d-2)}}\,, \tag{52}$$

where d is the space-time dimension, s_0 is a positive constant, and $\hat{n}$ is an outward pointing vector normal to ∂A. The EMI model has the interesting property that the mutual information, $I(A,B) = S(A) + S(B) - S(A\cup B)$, satisfies the extensivity property:

$$I(A, B\cup C) = I(A,B) + I(A,C)\,, \tag{53}$$

hence its name.

The entanglement entropy given by (52) is valid in flat space without boundaries. We introduce the following generalization that includes a flat boundary $\partial\mathcal{M}$ by the following simple ansatz, which we dub "bEMI:"

$$S_{\rm bEMI}(A) = \frac{1}{2} S_{\rm EMI}(A\cup A')\,, \tag{54}$$

where A' is the mirror image of A with respect to $\partial\mathcal{M}$, see Fig. 7. By construction, $S_{\rm bEMI}$ satisfies (4) with identical boundary conditions $\mathcal{B} = \mathcal{B}'$, although we are being agnostic about the physical meaning of the boundary condition since we do not know what theory has an entanglement entropy given by the bEMI. Note that we refer to (52) and (54) as entanglement entropies, but keep in mind that the EMI and bEMI ansatzes can be extended to general Rényi entropies by replacing s_0 with $s_{0,n}$.

A. Corner entanglement in 2 + 1 dimensions

For the EMI model, the bulk corner function $a_{\rm EMI}(\theta)$ reads [51]

$$a_{\rm EMI}(\theta) = 2s_0(1 + (\pi-\theta)\cot\theta)\,. \tag{55}$$

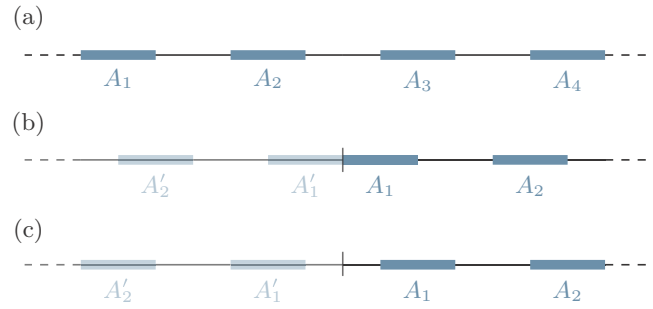

FIG. 7. Multi-interval entanglement for the (b)EMI model. (a) Four intervals on the infinite line without boundary. (b) Two intervals on the semi-infinite line, with A_1 connected to the boundary, and the mirror image through the boundary on the left. (c) Two intervals on the semi-infinite line, none connected to the boundary, and the mirror image through the boundary on the left.

Our bEMI ansatz thus yields the boundary corner function $b_{\rm EMI}(\theta)$:

$$b_{\rm EMI}(\theta) = \frac{1}{2} a_{\rm EMI}(2\theta)\,. \tag{56}$$

We note that this relation is identical to that of the free Dirac fermion (23) with mixed BCs, scalars with mixed BCs, and to the holographic one (19) with BCs $\alpha = \pi/2$. Using (55), we find that the boundary corner function vanishes at orthogonality $b_{\rm EMI}(\pi/2) = 0$, which implies the vanishing of the central charge

$$\mathfrak{a}^{\rm bEMI} = 0\,. \tag{57}$$

The expansion coefficients for angles near $\pi/2$ and 0 read $\sigma^{\rm bEMI} = s_0 4/3$ and $\kappa^{\rm bEMI} = s_0\pi/2$, respectively. These coefficients are listed in Table I. Using the known value [30] for the bulk theory, $C_T = s_0 16/\pi^2$, we see that the following relation holds:

$$\sigma^{\rm bEMI} = \frac{\pi^2}{12} C_T\,, \tag{58}$$

which is also satisfied by a free Dirac fermion with mixed BCs, free scalars with Dirichlet-Neumann BCs, and holographic CFTs with $\alpha = \pi/2$. Now, assuming the relation $\sigma^{(\mathcal{B})} = -\pi A_T^{(\mathcal{B})}$ holds for the bEMI, we can extract the boundary central charge: $A_T^{\rm bEMI} = -s_0 4/(3\pi)$. We note that this value is the same as the one we would have obtained using $A_T^{\rm bEMI} = -\pi C_T/12$. However, since we do not know whether these relations hold for the bEMI, the value of A_T is a conjecture.

$b_{\rm EMI}(\theta)$ (normalized) is plotted as a function of θ in Fig. 8. As one may see in this figure, the normalized boundary corner functions for the bEMI, holography, fermions, and N + D scalars are hardly discernible. Universality seems to be at play here. Gaining a better understanding of this is of foremost importance.

B. (1 + 1)-dimensional systems

In $d = 2$, the two integrals in (52) should be replaced by a double sum over the set of endpoints p_i of the intervals for

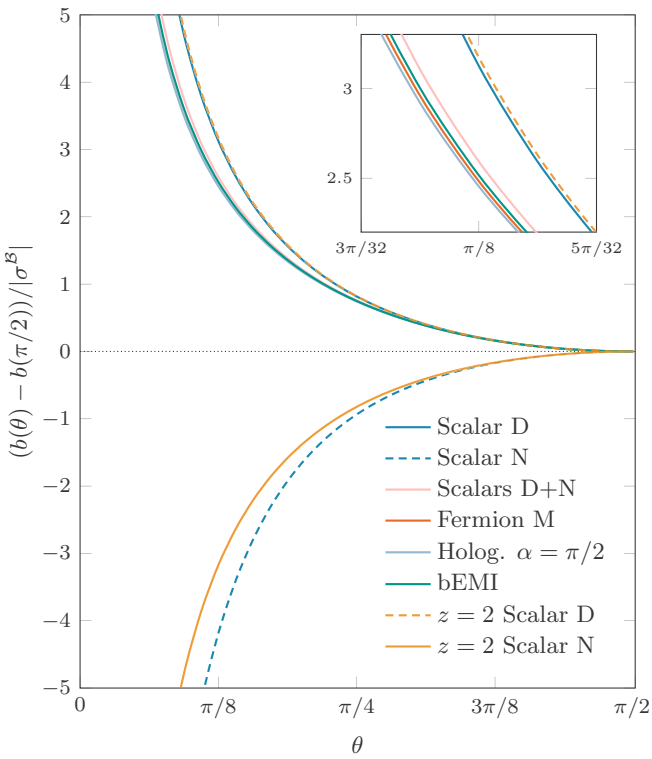

FIG. 8. Boundary corner entanglement for various theories. The boundary corner functions are normalized in such a way that near $\theta=\pi/2$ they behave as $b(\theta\simeq\pi/2)=\pm(\pi/2-\theta)^2$. The inset shows a closeup of the positive curves.

which the entropy is computed:

$$S_{\rm EMI}(A_1\cup A_2\cup\cdots)=-s_0\sum_{i,j}\hat{n}_i\cdot\hat{n}_j\ln|p_i-p_j|\,. \tag{59}$$

At coincidental points $p_i=p_j$, the expression above needs to be regulated; we thus introduce a short-distance UV cutoff ϵ, i.e., $|p_i-p_i|\to\epsilon$. Let us denote the set of endpoints by $\{p_i\}\equiv\{u_i,v_i\}$, where u_i and v_i are the left and right endpoints of the interval A_i, respectively. In the basis $(0,\hat{e}_x)$ with the unit vector $\hat{e}_x$ in the direction of increasing x, the normal vectors $\hat{n}_i$ at p_i are simply $\hat{n}_i=\pm\hat{e}_x$, depending on the endpoint being left $(-)$ or right $(+)$. It is then straightforward to show that the p-intervals entropy for the EMI model in $1+1$ dimensions takes the form

$$S_{\rm EMI}(A_1\cup A_2\cup\cdots\cup A_p)=2s_0\ln\left(\frac{\prod_{i,j}|u_i-v_j|}{\epsilon^p\prod_{i<j}|u_i-u_j||v_i-v_j|}\right). \tag{60}$$

Setting $s_0=\frac{1}{12}(1+\frac{1}{n})$, the entropy (60) is exactly the n-Rényi entropy of a free massless Dirac fermion [50]!

Our bEMI ansatz (54) for p regions yields

$$S_{\rm bEMI}(A_1\cup\cdots\cup A_p)=\tfrac{1}{2}S_{\rm EMI}(A'_p\cup\cdots\cup A'_1\cup A_1\cup\cdots\cup A_p)\,. \tag{61}$$

In particular, for one interval of length ℓ connected to the boundary in $1+1$ dimensions, Eq. (61) gives

$$S_{\rm bEMI}(\ell)=\frac{1}{12}\left(1+\frac{1}{n}\right)\ln\frac{2\ell}{\epsilon}\,, \tag{62}$$

which is exactly the result (2) for a Dirac fermion (with Virasoro central charge $c=1$) on the semi-infinite line. For one interval of length ℓ at a distance d from the boundary, we obtain

$$S_{\rm bEMI}(\ell,d)=\frac{1}{12}\left(1+\frac{1}{n}\right)\ln\frac{4\ell^2d(\ell+d)}{\epsilon^2(\ell+2d)^2}\,, \tag{63}$$

which again perfectly agrees with the known result [27] for the free fermion in a semi-infinite system. Note that taking the limits $d\to\infty$ and $d\to0$, one recovers (1) and (2), respectively. We therefore conclude that the EMI and bEMI models are exact for free fermions in $1+1$ dimensions.

V. LIFSHITZ FIELD THEORY IN 2 + 1 DIMENSIONS

Lifshitz field theories (LFTs) are nonrelativistic theories which exhibit anisotropic scaling between space and time, with characteristic dynamical exponent $z\neq1$. In $2+1$ dimensions, the free Lifshitz real scalar theory with dynamical critical exponent $z=2$ enjoys many interesting features. The corresponding Euclidean action for the noncompact scalar φ in $d=3$ is

$$I_{\rm LFT}[\varphi]=\frac{1}{2}\int d^3x[(\partial_\tau\varphi)^2+(\nabla^2\varphi)^2]. \tag{64}$$

We have absorbed an inessential constant that would appear in front of the term with spatial derivatives by using field and coordinate rescalings. For this model, the ground-state wave functional is given in terms of the Euclidean action $I_{\rm CFT}[\varphi]$ of the *two-dimensional* CFT [53],

$$|\Psi\rangle=\frac{1}{\sqrt{Z}}\int[d\varphi]e^{-\frac{1}{2}I_{\rm CFT}[\varphi]}|\varphi\rangle\,, \tag{65}$$

where Z is the partition function of the CFT,

$$Z=\int[d\varphi]e^{-I_{\rm CFT}[\varphi]}\,,\quad I_{\rm CFT}[\varphi]=\frac{1}{2}\int d^2x\,(\nabla\varphi)^2. \tag{66}$$

The ground-state wave function (65) of the $z=2$ free scalar is thus conformally invariant in space [53]!

We consider spatial bipartitions such as those shown in Fig. 2. Then, provided φ is noncompact, the Rényi entanglement entropy for the ground state is given by [24]

$$S_n=-\ln\frac{Z_AZ_B}{Z_{A\cup B}}\,, \tag{67}$$

and is independent of the Rényi index n, which we henceforth drop. Z_A and Z_B are the free (CFT) scalar partition functions on regions A and B, respectively, with continuity of the fields requiring Dirichlet BCs on the entangling curve Σ. $Z_{A\cup B}$ is the partition function on the entire space $\mathcal{M}$, with specified boundary conditions, e.g., Dirichlet or Neumann BCs, on the space boundary $\partial\mathcal{M}$. In Ref. [24], only Dirichlet BCs were considered. The entanglement entropy can thus be written as the difference in free energies

$$S=F_A+F_B-F_{A\cup B}\,. \tag{68}$$

For the free scalar field, the free energy can be expressed in terms of the heat kernel $K(s) \equiv e^{s\Delta}$ of the ($2d$ in our case) Laplacian operator Δ,

$$F = -\frac{1}{2}\int_{\epsilon^2}^{\infty} \frac{ds}{s} \operatorname{tr} K(s)\,, \tag{69}$$

where the trace is taken over the region of interest and $\epsilon \to 0$. Computing the entanglement entropy (68) thus boils down to computing the trace of the heat kernel on the three domains A, B, and $A \cup B$.

A. Corner entanglement for the $z = 2$ scalar

Suppose a two-dimensional domain $\mathcal{M}$ has a piecewise smooth boundary $\cup_i \partial\mathcal{M}_i$ consisting of a number of $\partial\mathcal{M}_i$ (with extrinsic curvature k_i) which may intersect at some points, the corners. Either Dirichlet or Neumann BC is imposed on each of the pieces $\partial\mathcal{M}_i^{D/N}$, thus yielding three types of corners (NN, DD, and ND). The heat trace $\operatorname{tr} K(s)$ admits an asymptotic expansion as $s \to 0$ of the form[4]:

$$\operatorname{tr} K(s) \simeq \sum_{p\geqslant 0} \mathrm{a}_p\, s^{(p-2)/2}\,, \tag{70}$$

where the coefficients a_p depend on the geometry of the domain and on the boundary conditions. Plugging the heat trace expansion in (69) yields the following leading terms in the free energy:

$$F = -\frac{\mathrm{a}_0}{2\epsilon^2} - \frac{\mathrm{a}_1}{\epsilon} - \mathrm{a}_2 \ln\frac{\ell}{\epsilon} + \mathcal{O}(1), \tag{71}$$

where ℓ is a length scale characteristic of the size of the domain on which the free energy is computed. The first three heat coefficients are given by (see Ref. [55] and references therein)

$$\mathrm{a}_0 = \frac{1}{4\pi}\int_{\mathcal{M}} 1\,, \tag{72}$$

$$\mathrm{a}_1 = \frac{1}{8\sqrt{\pi}}\left(\sum_i \int_{\partial\mathcal{M}_i^N} 1 - \sum_j \int_{\partial\mathcal{M}_j^D} 1\right), \tag{73}$$

$$\mathrm{a}_2 = \frac{1}{24\pi}\left(\int_{\mathcal{M}} R + \sum_i \int_{\partial\mathcal{M}_i} 2k_i\right) + \sum_j f_H(\theta_j) + \sum_k f_M(\theta_k)\,, \tag{74}$$

where we have defined the following heat corner functions:

$$f_H(\theta) = \frac{1}{24}\left(\frac{\pi}{\theta} - \frac{\theta}{\pi}\right), \tag{75}$$

$$f_M(\theta) = -\frac{1}{48}\left(\frac{\pi}{\theta} + \frac{2\theta}{\pi}\right), \tag{76}$$

[4]This classical asymptotic expansion of the heat trace may break down at the $p = 3$ level when considering the N/D problem (e.g., corners with mixed BCs), see Ref. [54]. However, we are only interested in the heat coefficients up to $p = 2$.

where H stands for a corner with homogenous BCs (DD or NN) and M for a mixed corner (ND). Note that the mixed heat corner coefficient can be obtained by applying relation (18), that is

$$f_H(2\theta) = f_H(\theta) + f_M(\theta)\,. \tag{77}$$

One can explicitly check (76) by computing the heat trace on mixed wedges of opening angles, e.g., $\pi/2$, $\pi/4$, $\pi/6$ with the method of images. This result for the mixed corner was previously obtained with the same arguments by Dowker in Ref. [56]. Notice that $f_M(\theta)$ is not a monotonic function of θ over $[0, \pi]$ as $f_H(\theta)$.

Getting back on track, it is clear that the volume terms, i.e., the a_0's, do not contribute to the entropy, while the boundary terms a_1 produce the area law (due to the Dirichlet BC imposed on the entangling surface). The first two (smooth) terms in a_2 do not contribute to the entropy either. However, the last two terms in a_2, originating from the corners, give rise to a logarithmic scaling in the entropy. The corner functions corresponding to the geometries in Fig. 2 are easily obtained by summing the heat coefficients $f_{H/M}$ for the regions A and B and subtracting those for $A \cup B$. The entanglement entropy for the $z = 2$ free scalar field thus has the following form:

$$S = B\frac{\ell}{\epsilon} - s_{\log} \ln\frac{\ell}{\epsilon} + \mathcal{O}(1)\,, \tag{78}$$

where the logarithmic coefficient $s_{\log}$ is given by the different corner functions,

$$s_{\log} = \sum_i a_{z=2}(\theta_i) + \sum_j b_{z=2}(\theta_j)\,. \tag{79}$$

Below we give formulas for these corner functions which will allow us to explicitly check our conjecture (4) for this theory.

1. Bulk corner

The well-known [24] bulk corner function $a_{z=2}(\theta)$ for the wedge does not depend on the boundary conditions on $\partial\mathcal{M}$ and reads for the $z = 2$ free scalar:

$$a_{z=2}(\theta) = \frac{(\pi-\theta)^2}{12\theta(2\pi-\theta)}\,, \tag{80}$$

which implies that the smooth- and cusp-limit coefficients respectively read [57]

$$\sigma = 1/(12\pi^2)\,, \quad \kappa = \pi/24\,. \tag{81}$$

2. Boundary corner

The boundary corner function $b_{z=2}(\theta)$ depends on the boundary condition imposed on $\partial\mathcal{M}$ (either D or N),

$$b_{z=2}^{(D)}(\theta) = \frac{1}{24}\left(\frac{\pi-\theta}{\theta} + \frac{\pi}{\pi-\theta}\right), \tag{82}$$

$$b_{z=2}^{(N)}(\theta) = -\frac{1}{48}\left(\frac{\pi+2\theta}{\theta} + \frac{\pi}{\pi-\theta}\right), \tag{83}$$

with

$$b_{z=2}^{(D)}(\pi/2) = -b_{z=2}^{(N)}(\pi/2) = 1/8\,, \tag{84}$$

$$\sigma^D = -2\sigma^N = 2/(3\pi^2)\,, \tag{85}$$

$$\kappa^D = -2\kappa^N = \pi/24\,. \tag{86}$$

These coefficients are listed in Table I. The two functions $b^{(D,N)}_{z=2}$ display the same qualitative behaviors as their relativistic cousins. Indeed, $b^{(D)}_{z=2}$ is a positive convex function of θ as $b^{(D)}_s$, while $b^{(N)}_{z=2}$ is negative and concave as $b^{(N)}_s$, as may be seen in Fig. 8. Surprisingly, the normalized functions $b^{(D)}_s$ and $b^{(D)}_{z=2}$ plotted in Fig. 8 coincide almost perfectly. This is unexpected given how different the two theories are (relativistic-conformal versus nonrelativistic). However, such an agreement does not occur for Neumann BC.

Remarkably, the corner functions for the $z = 2$ free scalar satisfy the same conjectured equality (22) as for the free relativistic scalar field,

$$a_{z=2}(2\theta) = b^{(D)}_{z=2}(\theta) + b^{(N)}_{z=2}(\theta)\,. \tag{87}$$

This exact result gives us further confidence in the validity of (4) and (18) for certain QFTs.

VI. MASSIVE THEORIES

So far, we have only considered gapless theories. However, many QFTs are not gapless, and so it is highly desirable to understand the fate of our bulk-boundary relation in that case. For one, we expect our relation (4) between bulk and boundary entropies to hold for certain free massive theories. As an example, let us take the free massive scalar field. The arguments presented in Sec. II B should carry through to the massive case. Indeed, the heat kernel for a massive scalar field is simply obtained from the massless case as $K^{(m)} = e^{-m^2 s} K^{(m=0)}$, such that $K^{(m)} = K^{(m)}_N + K^{(m)}_D$ holds. One could also repeat the treatment for the (half) disk geometry in Sec. III D 1 for the massive case. The Hamiltonian (33) with a mass term is obtained by replacing $k^2 \to k^2 + m^2$, thus relation (37) also holds for free massive scalars.

In the half-space, for a flat entangling surface that intersect orthogonally the physical boundary, the corresponding entanglement entropy can be computed explicitly in any dimensions [17]. For instance, in $3d$ one has

$$S^{(m)}_{D/N} = B\frac{\ell}{\epsilon} \pm \frac{1}{24}\ln(\epsilon m) + \cdots\,, \tag{88}$$

which satisfies the bulk-boundary relation (4): the logarithms cancel when we add the entropies corresponding to the two boundary conditions. The ellipsis represents terms subleading in ϵ; ℓ is the IR cutoff for the size of the entangling region.

The case of massive Dirac fermions must be treated with care because gapless edge states can be present on the boundary, which would arise in the description of Chern or Z_2 topological insulators, for instance. These gapless edge modes can affect the entanglement entropy of regions touching the boundary. We leave the discussion of such effects for future work.

VII. CONCLUSION

We studied the quantum entanglement properties of systems in the presence of a physical boundary. We have proposed a bulk-boundary relation (4) relating the Rényi entropies of certain theories with and without a boundary. Our attention was focused on situations where the entangling surface intersects the boundary of the space. In particular, in three dimensions, this leads to a new type of corner, called a boundary corner, from which originates new kinds of universal quantities in the entanglement entropy. These corner-induced logarithmic terms are not to be confused with those arising in the bulk when the entangling surface presents a singularity. For a given theory, the corresponding boundary corner function $b^{(\mathcal{B})}(\theta)$ depends on the opening angle θ of the corner adjacent to the physical boundary and on the boundary conditions $\mathcal{B}$. Our bulk-boundary relation connects the universal bulk and boundary corner terms for a family of theories (18). The relation applies for boundary theories with "mixed" BCs, such that for bCFTs the Euler boundary central charge vanishes $\mathfrak{a} = 0$, see (8). This is the case for free scalars evenly split between Dirichlet and Neumann BCs, as well as free Dirac fermions with mixed BCs, holographic CFTs with an $\alpha = \pi/2$ BC, and the boundary Extensive Mutual Information Model (bEMI). The latter allows a simple geometric calculation of the entanglement entropy in the presence of a flat boundary, and thus constitutes a very useful tool.

We also studied the Lifshitz free scalar with dynamical exponent $z = 2$. The bulk and boundary corner functions can be computed explicitly, producing remarkably simple functions of the opening angle θ for both Dirichlet and Neumann BCs. These functions satisfy the bulk-boundary relation (18), and behave very similarly to the case of the relativistic scalar. In particular, the Neumann corner function (83) is negative for all angles, just as in the relativistic case.

An interesting direction would be to study the relation between the bulk and boundary entanglement entropies of other Lifshitz theories and CFTs, such as the Ising CFT or its $N > 1$ cousins [generally known as $O(N)$ Wilson-Fisher fixed points]. In tour-de-force numerical calculations, the bulk corner function $a(\theta)$ for angles of $\pi/2$ was studied on the lattice [28,58–60], and analytically in the large-N limit [61]. It would be worthwhile to apply these methods to corners adjacent to the boundary, for different boundary conditions.

Our results also generalize to higher dimensions. For instance, we discuss the case of cylindrical entangling regions in $3 + 1$ dimensions in Appendix B. More interestingly, one could study the case of trihedral vertices, where three planes meet at a point. These vertices lead to a logarithmic contribution to the entanglement entropy for gapless theories, and were studied recently in the bulk for critical states [33,62–65], but much remains unknown about their properties. One could examine how the bulk trihedral entropy relates to that of boundary trihedral corners, where the two planes forming the entangling surface intersect the flat physical boundary to form a trihedral vertex.

ACKNOWLEDGMENTS

We would like to thank Sergueï Tchoumakov for useful discussions, and his assistance with the computing cluster. We also acknowledge interesting discussions with Jacopo Sisti and Jia Tian. C.B. thanks the Université de Montréal for warm hospitality during the completion of this project. C.B. was supported in part by the National Natural Science Foundation of China (NSFC, Grants No. 11335012, No. 11325522, and No. 11735001), and by a Boya Postdoctoral Fellowship at Peking University. W.W.-K. was funded by the Fondation

Courtois, a Discovery Grant from NSERC, a Canada Research Chair, and a "Établissement de nouveaux chercheurs et de nouvelles chercheuses universitaires" grant from FRQNT. This research was enabled in part by support provided by Calcul Québec [66] and Compute Canada [67].

APPENDIX A: COMMENTS ON BULK AND BOUNDARY CHARGES

Boundary conformal field theories offer a wider bestiary of central charges than conformal field theories. This has of course to be imputed to the presence of the "b" in bCFT. In three dimensional space-times with boundaries, the conformal anomaly no longer vanishes and there are two boundary charges, $\mathfrak{a}$ and c [68,69]. The vacuum expectation value of the trace of the stress tensor integrated over the space-time reads

$$\int_{\mathcal{M}_3} \langle T^\mu_\mu \rangle = -\frac{\mathfrak{a}}{96}\chi[\partial\mathcal{M}_3] + \frac{c}{256\pi}\int_{\partial\mathcal{M}_3} \mathrm{tr}\,\hat{k}^2, \tag{A1}$$

where $\chi[\partial\mathcal{M}_3]$ is the Euler characteristic of the boundary and $\hat{k}_{\mu\nu}$ is the traceless part of the extrinsic curvature tensor of the boundary. The charge c is independent of boundary conditions for free fields, while $\mathfrak{a}$ for scalars is not. For a free scalar field, $c = 1$ and $\mathfrak{a} = \pm 1$ for Dirichlet (+) and Neumann (−) boundary conditions, and $c = 2$, $\mathfrak{a} = 0$ for a free Dirac fermion with mixed boundary conditions. Recently [48,70], c has been connected to two other boundary charges, namely A_T and c_{nn}, where c_{nn} is the charge in the two-point function of the displacement operator. Then, with Eq. (50) which relates A_T to C_T for free fields, one finds that all the boundary charges presented above, with the exception of $\mathfrak{a}$, are related to the bulk charge C_T,

$$A_T = -\frac{c}{128\pi} = -\frac{\pi}{16}c_{nn} = -\frac{\pi}{12}C_T\,. \tag{A2}$$

Therefore only the boundary charge $\mathfrak{a}$ and the bulk charge C_T are independent for free fields. One may also wonder if such a relation between A_T and C_T exists in higher dimensions. For scalars, fermions and vectors we find in the literature [36,48,71,72]

$$C_T^s = \frac{d}{d-1}\frac{\Gamma^2(d/2)}{4\pi^d}\,, \qquad A_T^s = -\frac{\Gamma(d/2)}{2^d\pi^{d/2}(d^2-1)}\,, \tag{A3}$$

$$C_T^f = \frac{2^{\lfloor d/2\rfloor}d}{8\pi^d}\Gamma^2(d/2)\,, \quad A_T^{f(4d)} = -\frac{1}{40\pi^2}\,, \tag{A4}$$

$$C_T^{v(4d)} = \frac{4}{\pi^4}\,, \qquad A_T^{v(4d)} = -\frac{1}{20\pi^2}\,. \tag{A5}$$

For scalars, one gets in d dimensions

$$A_T = -\frac{2^{2-d}\pi^{d/2}}{d(d+1)\Gamma(d/2)}C_T\,. \tag{A6}$$

One can check that (A6) is actually satisfied for every known values of C_T and A_T for free CFTs. As an interacting example, for holographic bCFTs, we have in d dimensions [22],

$$A_{T,E}^{(\alpha)} = -\frac{L_{\mathrm{AdS}}^{d-1}}{8\pi G}\Bigg[\frac{1}{\cos\alpha}\,{}_2F_1(-1/2,(2-d)/2;1/2;\cos^2\alpha) - \frac{\sin^{d-2}\alpha}{\cos\alpha} + \frac{\sqrt{\pi}\,\Gamma(d/2)}{\Gamma\left(\frac{d-1}{2}\right)}\Bigg]^{-1}, \tag{A7}$$

$$C_{T,E} = \frac{L_{\mathrm{AdS}}^{d-1}}{8\pi G}\frac{(d+1)!}{(d-1)\pi^{d/2}}\frac{1}{\Gamma(d/2)}\,, \tag{A8}$$

and it is easy to show that for $\alpha = \pi/2$, we have

$$A_{T,E}^{(\pi/2)} = -\frac{2^{2-d}\pi^{d/2}}{d(d+1)\Gamma(d/2)}C_{T,E}\,, \tag{A9}$$

which is exactly (A6).

In $d = 4$ bCFTs, the conformal anomaly reads [7,69]

$$\int_{\mathcal{M}_4}\langle T\rangle = -\frac{a}{180}\chi[\mathcal{M}_4] + \frac{c}{1920\pi^2}\int_{\mathcal{M}_4} W^2_{\mu\nu\alpha\beta} - \frac{b_1}{240\pi^2}\int_{\partial\mathcal{M}_4}\hat{k}^{\mu\nu}W_{\mu nn\nu} + \frac{b_2}{280\pi^2}\int_{\partial\mathcal{M}_4}\mathrm{Tr}\,\hat{k}^3\,. \tag{A10}$$

The coefficients b_1 and b_2 are new boundary central charges while a and c are the well-known bulk charges. Only b_2 depends on boundary conditions as one finds from free fields $b_1 = c$. The values of these charges for free fields are given by

$$a^s = 1\,, \qquad a^f = 11\,, \quad a^v = 62\,, \tag{A11}$$

$$c^s = 1\,, \qquad c^f = 6\,, \quad c^v = 12\,, \tag{A12}$$

$$b_2^{s,D(N)} = 1\,(7/9)\,, \quad b_2^f = 5\,, \quad b_2^v = 8\,. \tag{A13}$$

It is known that $b_1 = c = 3\pi^4 C_T$ for free fields. In Ref. [39], it was proven that b_1 is related to the coefficient c_{nn} in the displacement operator two-point function as $b_1 = 2\pi^4 c_{nn}$. Further, in Ref. [48], b_1 has been connected to A_T via $b_1 = -240\pi^2 A_T$. Thus through this chain of relations for b_1, we have for free fields

$$A_T = -\frac{\pi^2}{120}c_{nn} = -\frac{b_1}{240\pi^2} = -\frac{\pi^2}{80}C_T\,. \tag{A14}$$

The last equality involving A_T and C_T is exactly relation (A6) for $d = 4$. Interestingly, the coefficient c_{nn} in d dimensions has been related to A_T in Ref. [73],

$$A_T = -\frac{d\,\pi^{(d-1)/2}}{d-1}\frac{\Gamma\left(\frac{d-1}{2}\right)}{\Gamma(d+2)}\,c_{nn}\,, \tag{A15}$$

where $c_{nn}^s = \frac{\Gamma^2(d/2)}{2\pi^d}$ for free scalars [38]. Then one can use (A6) to predict the value $c_{nn}^f = \frac{d-1}{4\pi^d}2^{\lfloor d/2\rfloor}\Gamma^2(d/2)$ for fermions in any dimensions. This last expression agrees with the known values for fermions in $d = 3$, 4 dimensions.

APPENDIX B: CYLINDERS IN $d = 4$ DIMENSIONS

Let us consider the entanglement entropy of a scalar field in a cylinder of length $L/2$ and radius $R \ll L$, anchored orthogonally on the flat boundary of the space $\partial\mathcal{M}$, as depicted in Fig. 9. We use cylindrical coordinates (r, θ, z). We may

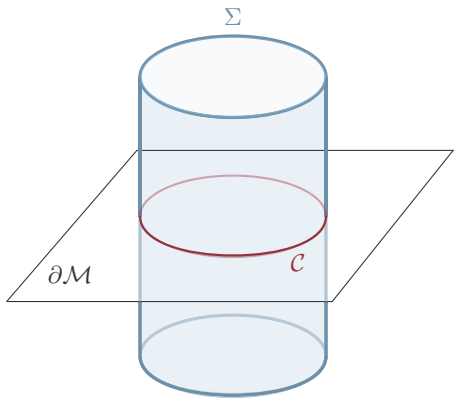

FIG. 9. $(3+1)$-dimensional space-time (time slice). The entangling surface Σ is a two-dimensional cylinder orthogonal to the boundary $\partial\mathcal{M}$. Their intersection (red) is a circle.

impose either Dirichlet or Neumann BCs on the boundaries at $z = 0,\ L/2$. In a similar manner as for the disk, we can dimensionally reduce our problem from $3+1$ to $1+1$ dimensions. To that end, the fields are decomposed in angular and axial modes as

$$\varphi(r,\theta,z) = \frac{1}{\sqrt{r}}\sum_{kl} f_{kl}(\theta,z)\,\varphi_{kl}(r)\,, \tag{B1}$$

$$\pi(r,\theta,z) = \frac{1}{\sqrt{r}}\sum_{kl} f_{kl}(\theta,z)\,\pi_{kl}(r)\,, \tag{B2}$$

where $f_{kl}(\theta,z)$ is a set of orthonormal functions which depend on the BCs such that

$$f^{(D)}_{kl}(\theta,z) = \frac{1}{\sqrt{\pi L}} e^{il\theta}\sin(2\pi kz/L), \quad k = 1,2,\dots, \tag{B3}$$

$$f^{(N)}_{kl}(\theta,z) = \frac{1}{\sqrt{\pi L}} e^{il\theta}\cos(2\pi kz/L), \quad k = 0,1,\dots, \tag{B4}$$

and $l \in \mathbb{Z}$. The Hamiltonian can then be written as $H = \sum_{kl} H_{kl}$, where

$$H_{kl} = \frac{1}{2}\int dr\left(\pi_{kl}^2 + r\partial_r\left(\frac{\varphi_{kl}}{\sqrt{r}}\right)^2 + \left(\frac{l^2}{r^2}+\omega_k^2\right)\varphi_{kl}^2\right), \tag{B5}$$

and $\omega_k = 2\pi k/L$. The entanglement entropies for Dirichlet and Neumann BCs are thus given by

$$S^{(D)}_{\rm cyl}(R) = \sum_{l=-\infty}^{\infty}\sum_{k=1}^{\infty} S_{kl}\,, \tag{B6}$$

$$S^{(N)}_{\rm cyl}(R) = \sum_{l=-\infty}^{\infty}\sum_{k=0}^{\infty} S_{kl}\,, \tag{B7}$$

where S_{kl} is the entropy associated to H_{kl}.

Now, we want to compute the entanglement entropy of a cylinder of length L and radius $R \ll L$ (no boundary here). It is convenient to compactify the direction z by imposing periodic BCs $z = z + L$ and decompose the fields on axial and angular modes with eigenfunctions $f_{kl}(\theta,z) = \frac{1}{\sqrt{2\pi L}} e^{il\theta} e^{i2\pi kz/L}$, where $k, l \in \mathbb{Z}$. The entanglement entropy of a cylinder is thus given by

$$S_{\rm cyl}(R) = \sum_{k,l=-\infty}^{\infty} S_{kl}\,, \tag{B8}$$

which can be written as

$$S_{\rm cyl}(R) = S^{(D)}_{\rm cyl}(R) + S^{(N)}_{\rm cyl}(R)\,, \tag{B9}$$

as for the disk case.

Again, it is interesting that the difference between the entanglement entropy for Dirichlet and Neumann BCs is the presence of the $k = 0$ mode in the latter. One further notices that the entropy associated to this mode is in fact the entropy of a scalar field in a disk of radius R in $2+1$ dimensions (36), and we have

$$S^{(N)}_{\rm cyl}(R) = S^{(D)}_{\rm cyl}(R) + S_{\rm disk}(R)\,. \tag{B10}$$

The equality (B10) yields the following relation for the logarithmic contributions $s_{\rm cyl}$:

$$s^{(N)}_{\rm cyl} = s^{(D)}_{\rm cyl}\,, \tag{B11}$$

as there is no logarithmic contribution for the disk in $2+1$ dimensions. Equation (B11) is actually the expected result for the cylinder. In a flat four-dimensional space-time with a flat boundary $\partial\mathcal{M}$, the logarithmic term in the entanglement entropy for an entangling surface Σ intersecting orthogonally the boundary is given by [74,75]

$$s_{\log} = \frac{a}{180}\chi[\Sigma] + \frac{c}{240\pi}\int_\Sigma \mathrm{tr}\,\hat{k}_i^2\,.$$

The first term is the Euler characteristic of Σ and $(\hat{k}_i)_{\mu\nu}$ is the traceless part of the extrinsic curvature of Σ as embedded in the four-dimensional space-time. The central charges a and c do not depend on the BCs. The Euler characteristic of a cylinder (with a geodesic boundary or none) is zero and only the c part in the logarithmic contribution remains.

A similar calculation for an hemisphere would yield the same relations as (B9) and (B11), only for the (hemi)sphere, it is the a part that is nonvanishing. Note that $\chi[\text{sphere}] = 2$ and $\chi[\text{hemisphere}] = 1$.

APPENDIX C: IMPLEMENTATION OF BOUNDARY CONDITIONS FOR THE DISCRETIZED SCALAR FIELD

The continuum Hamiltonian of a free massless scalar field in $1+1$ space-time dimensions is

$$H = \frac{1}{2}\int dx\big(\pi^2 + \phi\big(-\partial_x^2\big)\phi\big)\,. \tag{C1}$$

In the discrete case, the fields are evaluated at a lattice site $i \in [1,N]$ such that $\phi(x) \to \phi(x_i) \equiv \phi_i$ and $\pi(x) \to \pi(x_i) \equiv \pi_i$. The above Hamiltonian is thus replaced by

$$H = \frac{1}{2}(\pi^T\pi + \phi^T K\phi)\,, \tag{C2}$$

where $\phi^T = (\phi_1,\phi_2,\cdots,\phi_N)$, $\pi^T = (\pi_1,\pi_2,\cdots,\pi_N)$, and the matrix K is the discretized version of the spatial Laplacian operator $-\partial_x^2$. In the static case, the Hamiltonian (C2) yields the equations of motion

$$K\phi = 0\,, \tag{C3}$$

with specified boundary conditions at both ends of the lattice. Since we are considering a scalar field, its discrete counterpart is the harmonic chain with nearest neighbors interactions. The equation of motion for the oscillator ϕ_i reads

$$-\phi_{i-1} + 2\phi_i - \phi_{i+1} = 0\,. \tag{C4}$$

One should however take the boundary conditions into account in the equations of motion of ϕ_1 and ϕ_N. In order to implement boundary conditions on a discrete domain, we first introduce fictitious degrees of freedom, ϕ_0 and ϕ_{N+1}. The equations of motion for ϕ_1 and ϕ_N are

$$-\phi_0 + 2\phi_1 - \phi_2 = 0\,, \tag{C5}$$

$$-\phi_{N-1} + 2\phi_N - \phi_{N+1} = 0\,, \tag{C6}$$

but we can get rid of the extra ϕ_0 and ϕ_{N+1} by substituting in (C5) and (C6) boundary conditions such as

$$\text{Periodic}: \quad \phi_0 = \phi_N\,, \tag{C7}$$

$$\text{Dirichlet}: \quad \phi_0 = 0\,, \tag{C8}$$

$$\text{Neumann}: \quad \phi_1 - \phi_0 = 0\,, \tag{C9}$$

at $i = 0$, and similarly at $i = N + 1$. Then, the equations of motion including the boundary conditions are put in the vector form (C3), from which one can read off the matrix K. For example, with Dirichlet/Neumann BC on the left/right end, K is a tridiagonal $N \times N$ matrix,

$$K_{DN} = \begin{pmatrix} 2 & -1 & & & \\ -1 & 2 & -1 & & \\ & \ddots & \ddots & \ddots & \\ & & -1 & 2 & -1 \\ & & & -1 & 1 \end{pmatrix}. \tag{C10}$$

The matrix K has eigenvectors $v_{i,j}$ (i labels the components of jth eigenvector) and eigenvalues $\omega_j^2 = 4\sin^2(k_j/2)$ where k_j depends on the BCs:

$$\text{P}: k_j = \frac{2\pi j}{N}\,, \qquad v_{i,j} = \frac{1}{\sqrt{N}}\exp(\imath k_j i)\,, \tag{C11}$$

$$\text{DD}: k_j = \frac{i\pi}{N+1}\,, \qquad v_{i,j} = \sqrt{\frac{2}{N+1}}\sin(k_j i)\,, \tag{C12}$$

$$\text{NN}: k_j = \frac{\pi(j-1)}{N}\,, \qquad v_{i,j} = \sqrt{\frac{2-\delta_{j,1}}{N}}\cos[k_j(i-1/2)]\,, \tag{C13}$$

$$\text{DN}: k_j = \frac{\pi(2j-1)}{2N+1}\,, \qquad v_{i,j} = \sqrt{\frac{2}{N+1/2}}\sin(k_j i), \tag{C14}$$

$$\text{ND}: k_j = \frac{\pi(2j-1)}{2N+1}, \qquad v_{i,j} = \sqrt{\frac{2}{N+1/2}}\cos[k_j(i-1/2)]\,. \tag{C15}$$

TABLE III. Smooth limit coefficients for the scalar bulk corner function $a_n(\theta)$ [46].

n	1	2
σ_n	$\frac{1}{256}$	$\frac{1}{48\pi^2}$
$\sigma_n^{(1)}$	$\frac{20+3\pi^2}{18432\pi^2}$	$\frac{5+\pi^2}{960\pi^4}$
$\sigma_n^{(2)} \times 10^5$	2.67327749	1.55767377
$\sigma_n^{(3)} \times 10^6$	2.70080311	1.56206308
$\sigma_n^{(4)} \times 10^7$	2.72879243	1.57369200
$\sigma_n^{(5)} \times 10^8$	2.75578382	1.58861117
$\sigma_n^{(6)} \times 10^9$	2.78590964	1.60561386
$\sigma_n^{(7)} \times 10^{10}$	2.81790229	1.62402979

Finally, we obtain the ground-state correlation functions for the scalar field on the lattice as

$$\langle\phi_i\phi_j\rangle = \frac{1}{2}K_{ij}^{-1/2} = \frac{1}{2}\sum_n \omega_n^{-1} v_{i,n} v_{j,n}^\dagger\,, \tag{C16}$$

$$\langle\pi_i\pi_j\rangle = \frac{1}{2}K_{ij}^{1/2} = \frac{1}{2}\sum_n \omega_n v_{i,n} v_{j,n}^\dagger\,. \tag{C17}$$

Note that for a massive field we have $\omega_n^2 \to \omega_n^2 + m^2$.

APPENDIX D: HIGH-PRECISION ANSATZ FOR THE SCALAR BULK CORNER FUNCTION

We present in this Appendix the high-precision ansatz of Ref. [46] for the scalar bulk corner function $a_n(\theta)$, where n is the Rényi index. This ansatz takes the form

$$a_n(\theta) \simeq \sum_{p=1}^{M} \sigma_n^{(p-1)}(\theta-\pi)^{2p} + \frac{2\kappa_n}{\pi^{2M+1}}\frac{(\theta-\pi)^{2(M+1)}}{\theta(2\pi-\theta)}\,, \tag{D1}$$

where M corresponds to the number of smooth limit coefficients $\sigma_n^{(p-1)}$ used ($\sigma_n^{(0)} \equiv \sigma_n$). We refer the reader to Ref. [41] for the details regarding the expansion of the corner function in the nearly smooth limit. We give in Table III the coefficients $\sigma_n^{(p-1)}$ up to $p = 8$ ($M = 8$) for $n = 1, 2$ found in Refs. [41,46]. For the cusp limit coefficients, the value of $\kappa \equiv \kappa_1$ is reported below Eq. (26), while the $n = 2$ one may be found in Ref. [40], $\kappa_2 = 0.0227998$.

[1] X. Wen, *Quantum Field Theory of Many-Body Systems: From the Origin of Sound to an Origin of Light and Electrons*, Oxford Graduate Texts (Oxford University Press, Oxford, 2007).

[2] H. W. Diehl, The Theory of boundary critical phenomena, Int. J. Mod. Phys. B **11**, 3503 (1997).

[3] P. Calabrese and J. L. Cardy, Entanglement entropy and quantum field theory, J. Stat. Mech. (2004) P06002.

[4] P. Calabrese and J. Cardy, Entanglement entropy and conformal field theory, J. Phys. A **42**, 504005 (2009).

[5] N. Laflorencie, E. S. Sorensen, M.-S. Chang, and I. Affleck, Boundary Effects in the Critical Scaling of Entanglement Entropy in 1D Systems, Phys. Rev. Lett. **96**, 100603 (2006).

[6] I. Affleck, N. Laflorencie, and E. S. Sorensen, Entanglement entropy in quantum impurity systems and systems with boundaries, J. Phys. A: Math. Theor. **42**, 504009 (2009).

[7] C. P. Herzog, K.-W. Huang, and K. Jensen, Universal entanglement and boundary geometry in conformal field theory, J. High Energy Phys. 01 (2016) 162.

[8] D. V. Fursaev and S. N. Solodukhin, Anomalies, entropy and boundaries, Phys. Rev. D **93**, 084021 (2016).

[9] H. Casini, I. S. Landea, and G. Torroba, The g-theorem and quantum information theory, J. High Energy Phys. 10 (2016)140.

[10] T. Zhou, X. Chen, T. Faulkner, and E. Fradkin, Entanglement entropy and mutual information of circular entangling surfaces in the $2+1$-dimensional quantum Lifshitz model, J. Stat. Mech. (2016) 093101.

[11] X. Chen, W. Witczak-Krempa, T. Faulkner, and E. Fradkin, Two-cylinder entanglement entropy under a twist, J. Stat. Mech. (2017) 043104.

[12] X. Chen, E. Fradkin, and W. Witczak-Krempa, Quantum spin chains with multiple dynamics, Phys. Rev. B **96**, 180402(R) (2017).

[13] R. C. Myers and A. Sinha, Seeing a c-theorem with holography, Phys. Rev. D **82**, 046006 (2010).

[14] R. C. Myers and A. Sinha, Holographic c-theorems in arbitrary dimensions, J. High Energy Phys. 01 (2011) 125.

[15] H. Casini and M. Huerta, On the RG running of the entanglement entropy of a circle, Phys. Rev. D **85**, 125016 (2012).

[16] H. Casini, I. Salazar Landea, and G. Torroba, Irreversibility in quantum field theories with boundaries, J. High Energy Phys. 04 (2019) 166.

[17] C. Berthiere and S. N. Solodukhin, Boundary effects in entanglement entropy, Nucl. Phys. B **910**, 823 (2016).

[18] C. Berthiere, Boundary-corner entanglement for free bosons, Phys. Rev. B **99**, 165113 (2019).

[19] T. Takayanagi, Holographic Dual of BCFT, Phys. Rev. Lett. **107**, 101602 (2011).

[20] M. Fujita, T. Takayanagi, and E. Tonni, Aspects of AdS/BCFT, J. High Energy Phys. 11 (2011) 043.

[21] A. Faraji Astaneh, C. Berthiere, D. Fursaev, and S. N. Solodukhin, Holographic calculation of entanglement entropy in the presence of boundaries, Phys. Rev. D **95**, 106013 (2017).

[22] D. Seminara, J. Sisti, and E. Tonni, Corner contributions to holographic entanglement entropy in $AdS_4/BCFT_3$, J. High Energy Phys. 11 (2017) 076.

[23] D. Seminara, J. Sisti, and E. Tonni, Holographic entanglement entropy in $AdS_4/BCFT_3$ and the Willmore functional, J. High Energy Phys. 08 (2018) 164.

[24] E. Fradkin and J. E. Moore, Entanglement Entropy of 2D Conformal Quantum Critical Points: Hearing the Shape of A Quantum Drum, Phys. Rev. Lett. **97**, 050404 (2006).

[25] H.-Q. Zhou, T. Barthel, J. O. Fjærestad, and U. Schollwöck, Entanglement and boundary critical phenomena, Phys. Rev. A **74**, 050305(R) (2006).

[26] I. Affleck and A. W. W. Ludwig, Universal Noninteger 'Ground State Degeneracy' in Critical Quantum Systems, Phys. Rev. Lett. **67**, 161 (1991).

[27] M. Fagotti and P. Calabrese, Universal parity effects in the entanglement entropy of XX chains with open boundary conditions, J. Stat. Mech. (2011) P01017.

[28] A. B. Kallin, K. Hyatt, R. R. P. Singh, and R. G. Melko, Entanglement at a Two-Dimensional Quantum Critical Point: A Numerical Linked-Cluster Expansion Study, Phys. Rev. Lett. **110**, 135702 (2013).

[29] T. Hirata and T. Takayanagi, AdS/CFT and strong subadditivity of entanglement entropy, J. High Energy Phys. 02 (2007) 042.

[30] P. Bueno, R. C. Myers, and W. Witczak-Krempa, Universality of Corner Entanglement in Conformal Field Theories, Phys. Rev. Lett. **115**, 021602 (2015).

[31] P. Bueno and R. C. Myers, Corner contributions to holographic entanglement entropy, J. High Energy Phys. 08 (2015) 068.

[32] T. Faulkner, R. G. Leigh, and O. Parrikar, Shape dependence of entanglement entropy in conformal field theories, J. High Energy Phys. 04 (2016) 088.

[33] W. Witczak-Krempa, Entanglement susceptibilities and universal geometric entanglement entropy, Phys. Rev. B **99**, 075138 (2019).

[34] S. Ryu and T. Takayanagi, Holographic Derivation of Entanglement Entropy from AdS/CFT, Phys. Rev. Lett. **96**, 181602 (2006).

[35] R. C. Myers and A. Singh, Entanglement entropy for singular surfaces, J. High Energy Phys. 09 (2012) 013.

[36] D. Deutsch and P. Candelas, Boundary effects in quantum field theory, Phys. Rev. D **20**, 3063 (1979).

[37] H. Luckock, Mixed boundary conditions in quantum field theory, J. Math. Phys. **32**, 1755 (1991).

[38] D. M. McAvity and H. Osborn, Energy momentum tensor in conformal field theories near a boundary, Nucl. Phys. B **406**, 655 (1993).

[39] C. P. Herzog and K.-W. Huang, Boundary conformal field theory and a boundary central charge, J. High Energy Phys. 10 (2017) 189.

[40] P. Bueno, R. C. Myers, and W. Witczak-Krempa, Universal corner entanglement from twist operators, J. High Energy Phys. 09 (2015) 091.

[41] H. Casini and M. Huerta, Entanglement entropy in free quantum field theory, J. Phys. A **42**, 504007 (2009).

[42] H. Casini and M. Huerta, Universal terms for the entanglement entropy in $2+1$ dimensions, Nucl. Phys. B **764**, 183 (2007).

[43] H. Casini, M. Huerta, and L. Leitao, Entanglement entropy for a Dirac fermion in three dimensions: Vertex contribution, Nucl. Phys. B **814**, 594 (2009).

[44] J. S. Dowker, Entanglement entropy for odd spheres, arXiv:1012.1548.

[45] J. S. Dowker, Entanglement entropy for even spheres, arXiv:1009.3854.

[46] J. Helmes, L. E. Hayward Sierens, A. Chandran, W. Witczak-Krempa, and R. G. Melko, Universal corner entanglement of Dirac fermions and gapless bosons from the continuum to the lattice, Phys. Rev. B **94**, 125142 (2016).

[47] C. De Nobili, A. Coser, and E. Tonni, Entanglement negativity in a two dimensional harmonic lattice: Area law and corner contributions, J. Stat. Mech. (2016) 083102.

[48] R.-X. Miao and C.-S. Chu, Universality for shape dependence of casimir effects from weyl anomaly, J. High Energy Phys. 03 (2018) 046.

[49] R.-X. Miao, Holographic BCFT with dirichlet boundary condition, J. High Energy Phys. 02 (2019) 025.

[50] H. Casini, C. D. Fosco, and M. Huerta, Entanglement and alpha entropies for a massive Dirac field in two dimensions, J. Stat. Mech. (2005) P07007.

[51] H. Casini and M. Huerta, Remarks on the entanglement entropy for disconnected regions, J. High Energy Phys. 03 (2009) 048.

[52] B. Swingle, Mutual information and the structure of entanglement in quantum field theory, arXiv:1010.4038.

[53] E. Ardonne, P. Fendley, and E. Fradkin, Topological order and conformal quantum critical points, Ann. Phys. **310**, 493 (2004).

[54] J. S. Dowker, P. B. Gilkey, and K. Kirsten, On properties of the asymptotic expansion of the heat trace for the N/D problem, Int. J. Math. **12**, 505 (2001).

[55] D. V. Vassilevich, Heat kernel expansion: User's manual, Phys. Rep. **388**, 279 (2003).

[56] J. S. Dowker, The N U D problem, arXiv:hep-th/0007129.

[57] P. Bueno and W. Witczak-Krempa, Bounds on corner entanglement in quantum critical states, Phys. Rev. B **93**, 045131 (2016).

[58] E. M. Stoudenmire, P. Gustainis, R. Johal, S. Wessel, and R. G. Melko, Corner contribution to the entanglement entropy of strongly interacting O(2) quantum critical systems in $2+1$ dimensions, Phys. Rev. B **90**, 235106 (2014).

[59] A. B. Kallin, E. M. Stoudenmire, P. Fendley, R. R. P. Singh, and R. G. Melko, Corner contribution to the entanglement entropy of an O(3) quantum critical point in $2+1$ dimensions, J. Stat. Mech. (2014) P06009.

[60] S. Sahoo, E. M. Stoudenmire, J.-M. Stephan, T. Devakul, R. R. P. Singh, and R. G. Melko, Unusual corrections to scaling and convergence of universal renyi properties at quantum critical points, Phys. Rev. B **93**, 085120 (2016).

[61] S. Whitsitt, W. Witczak-Krempa, and S. Sachdev, Entanglement entropy of large-N Wilson-Fisher conformal field theory, Phys. Rev. B **95**, 045148 (2017).

[62] T. Devakul and R. R. P. Singh, Entanglement across a cubic interface in $3+1$ dimensions, Phys. Rev. B **90**, 054415 (2014).

[63] L. E. Hayward Sierens, P. Bueno, R. R. P. Singh, R. C. Myers, and R. G. Melko, Cubic trihedral corner entanglement for a free scalar, Phys. Rev. B **96**, 035117 (2017).

[64] G. Bednik, L. E. Hayward Sierens, M. Guo, R. C. Myers, and R. G. Melko, Probing trihedral corner entanglement for Dirac fermions, Phys. Rev. B **99**, 155153 (2019).

[65] P. Bueno, H. Casini, and W. Witczak-Krempa, Generalizing the entanglement entropy of singular regions in conformal field theories, J. High Energy Phys. 08 (2019) 069.

[66] www.calculquebec.ca.

[67] www.computecanada.ca.

[68] C. R. Graham and E. Witten, Conformal anomaly of submanifold observables in AdS/CFT correspondence, Nucl. Phys. B **546**, 52 (1999).

[69] S. N. Solodukhin, Boundary Terms of Conformal Anomaly, Phys. Lett. B **752**, 131 (2016).

[70] C. Herzog, K.-W. Huang, and K. Jensen, Displacement Operators and Constraints on Boundary Central Charges, Phys. Rev. Lett. **120**, 021601 (2018).

[71] H. Osborn and A. C. Petkou, Implications of conformal invariance in field theories for general dimensions, Ann. Phys. **231**, 311 (1994).

[72] E. Perlmutter, A universal feature of CFT Rényi entropy, J. High Energy Phys. 03 (2014) 117.

[73] R.-X. Miao, Casimir effect, weyl anomaly and displacement operator in boundary conformal field theory, J. High Energy Phys. 07 (2019) 098.

[74] S. N. Solodukhin, Entanglement entropy, conformal invariance and extrinsic geometry, Phys. Lett. B **665**, 305 (2008).

[75] D. V. Fursaev, Quantum entanglement on boundaries, J. High Energy Phys. 07 (2013) 119